Spectral networks and Fenchel-Nielsen coordinates

Lotte Hollands[1] and Andrew Neitzke[2]

[1]Department of Mathematics, Heriot-Watt University
[2]Department of Mathematics, University of Texas at Austin

Abstract

It is known that spectral networks naturally induce certain coordinate systems on moduli spaces of flat $SL(K)$-connections on surfaces, previously studied by Fock and Goncharov. We give a self-contained account of this story in the case $K = 2$, and explain how it can be extended to incorporate the complexified Fenchel-Nielsen coordinates. As we review, the key ingredient in the story is a procedure for passing between moduli of flat $SL(2)$-connections on C (equipped with a little extra structure) and moduli of equivariant $GL(1)$-connections over a covering $\Sigma \to C$; taking holonomies of the equivariant $GL(1)$-connections then gives the desired coordinate systems on moduli of $SL(2)$-connections. There are two special types of spectral network, related to ideal triangulations and pants decompositions of C; these two types of network lead to Fock-Goncharov and complexified Fenchel-Nielsen coordinate systems respectively.

Mathematics Subject Classification: 54,53,81.
Keywords: spectral networks, flat connections, Darboux coordinates.

Contents

1 Introduction

In the recent paper [1] a process called *nonabelianization* is described. Nonabelianization and its inverse, abelianization, allow one to study flat connections in rank K vector bundles over a (perhaps punctured) surface C, by relating them to simpler objects, namely connections in rank 1 bundles over K-fold branched covers of C.

The main new result of this paper is that abelianization gives a new way of thinking about a classical object, namely the complexified *Fenchel-Nielsen coordinate system* on a certain covering of the moduli space of $PSL(2)$-connections over C.[1]

Before describing the main points of this paper, let us briefly review what is meant by (non)abelianization. Suppose given a flat $GL(1)$-connection ∇^{ab} in a complex line bundle over a branched cover Σ of C.[2] A naive way of relating ∇^{ab} to a rank K connection over C would be just to take the pushforward. This indeed gives a connection $\nabla = \pi_* \nabla^{\mathrm{ab}}$ in a rank K bundle over C, or more precisely over the complement of the branch locus in C. However, the connection $\pi_* \nabla^{\mathrm{ab}}$ does *not* extend smoothly over the branch locus. The reason is simple: when one goes around a branch point of the covering $\Sigma \to C$, the sheets of Σ are permuted, and this permutation shows up as a nontrivial monodromy for $\pi_* \nabla^{\mathrm{ab}}$. Thus $\pi_* \nabla^{\mathrm{ab}}$ cannot be extended to a flat connection on the whole of C.

The nonabelianization operation is a recipe for "fixing up" this monodromy problem, by cutting the surface C into pieces, then regluing with unipotent automorphisms of $\pi_* \nabla^{\mathrm{ab}}$ along the gluing lines. The effect of this cutting-and-gluing is to cancel the unwanted monodromy around branch points while not creating any monodromy anywhere else.

The cutting-and-gluing is done along a collection of paths on C, carrying some extra labels and obeying some conditions, called a *spectral network* $\mathcal{W}$. Spectral networks were described in [1], where it was shown that they are a fundamental ingredient in the story of BPS states and wall-crossing for $\mathcal{N} = 2$ supersymmetric quantum field theories of "class S" [2, 3]. For subsequent work on spectral networks in $\mathcal{N} = 2$ theories see [4, 5, 6, 7]. Essentially the same object has also been considered in the mathematical literature on Stokes phenomena, e.g. [8].

Fixing a spectral network $\mathcal{W}$ and given a generic flat $GL(1)$-connection ∇^{ab}, we can nonabelianize ∇^{ab}. We can also consider an inverse operation, abelianization: given a generic flat rank K connection ∇ over C, we attempt to realize it by cutting-and-gluing of $\pi_* \nabla^{\mathrm{ab}}$ along the spectral network $\mathcal{W}$, for some flat $GL(1)$-connection ∇^{ab}.

In this paper we formalize the (non)abelianization process, focussing on $K = 2$. We start with the definition of a spectral network in §2.1.[3] In the remainder of §2 and §3 we introduce various examples; in particular we introduce two classes of spectral networks, which we call *Fock-Goncharov* (which had been considered earlier, in [4]) and *Fenchel-Nielsen* networks (which are new), for a reason which will become apparent momentarily. Fock-Goncharov networks are dual to ideal triangulations, whereas Fenchel-Nielsen ones are related to pants decompositions of C.

§4 introduces the concept of $\mathcal{W}$-abelianization. We formulate this as an extension of a flat $SL(2)$-connection ∇ into a so-called $\mathcal{W}$-pair, which contains the connection ∇ in

[1] In this paper we always consider the *complex* groups, so $PSL(2)$ means $PSL(2, \mathbb{C})$ and $SL(2)$ means $SL(2, \mathbb{C})$.

[2] More precisely, it will turn out that we should consider $GL(1)$-connections with an additional equivariance property, as explained in §4.2 below, and as a consequence of this equivariance they will not be flat but rather have holonomy -1 around the branch locus of the covering $\Sigma \to C$; for the rest of this introduction we suppress this subtlety.

[3] For our purposes in this paper we do not need the most general notion of spectral network, in the case $K = 2$ things are simpler.

the "abelianized gauge" $\pi_* \nabla^{\mathrm{ab}}$. We explicitly construct $\mathcal{W}$-pairs for Fock-Goncharov and Fenchel-Nielsen networks in §5.

For the particular networks we consider in this paper, there is an almost unique way of $\mathcal{W}$-abelianizing a given generic connection ∇. "Almost unique" means that there are some discrete choices to be made, which in this paper we encapsulate in a notion of $\mathcal{W}$-*framed* connection; then, we find a canonical 1-1 correspondence between $\mathcal{W}$-framed flat $SL(2)$-connections ∇ over C and $\mathcal{W}$-abelianizations.

In the latter half of the paper we discuss $\mathcal{W}$-nonabelianization. Similarly, we formulate this as an extension of a flat $GL(1)$-connection ∇^{ab} into a $\mathcal{W}$-pair. For convenience later on, we do this in the language of parallel transport of the relevant connections. We explain the dictionary in §6. In §7 we introduce the notion of $\mathcal{W}$-nonabelianization and show that there is a canonical 1-1 correspondence between flat $GL(1)$-connections ∇^{ab} and $\mathcal{W}$-nonabelianizations when $\mathcal{W}$ is either a Fock-Goncharov or Fenchel-Nielsen type network. In §9 we discuss concrete examples.

We combine these two pieces in §8. Given any spectral network $\mathcal{W}$ there is a diagram

$$\begin{tikzcd} & \mathcal{M}(\mathcal{W}) & \\ \mathcal{M}(\Sigma, GL(1)) \arrow[ur, "\psi_1"] & & \mathcal{M}(C, SL(2), \mathcal{W}) \arrow[ul, "\psi_2"'] \end{tikzcd}$$

where $\mathcal{M}(\Sigma, GL(1))$ is the moduli space of flat $GL(1)$-connections, $\mathcal{M}(\mathcal{W})$ the moduli space of $\mathcal{W}$-pairs and $\mathcal{M}(C, SL(2), \mathcal{W})$ the moduli space of $\mathcal{W}$-framed $SL(2)$-connections. In this diagram ψ_1 denotes $\mathcal{W}$-nonabelianization and ψ_2 denotes $\mathcal{W}$-abelianization. Since we have shown that both maps ψ_1 and ψ_2 are bijections when $\mathcal{W}$ is a Fock-Goncharov or Fenchel-Nielsen type network, we obtain another bijective map

$$\Psi_{\mathcal{W}} : \mathcal{M}(C, SL(2), \mathcal{W}) \to \mathcal{M}(\Sigma, GL(1)). \tag{1.1}$$

The relation to coordinate systems now comes about as follows. Given a $\mathcal{W}$-framed connection ∇ and some $\gamma \in H_1(\Sigma, \mathbb{Z})$, let $\mathcal{X}_\gamma(\nabla) \in \mathbb{C}^\times$ denote the holonomy around γ of the corresponding $GL(1)$-connection ∇^{ab}. For the networks $\mathcal{W}$ we consider in this paper, the collection of numbers $\mathcal{X}_\gamma(\nabla)$ suffice to determine the connection ∇. In these cases, we thus get a coordinate system on the moduli space of $\mathcal{W}$-framed flat connections ∇; call this the *spectral coordinate system* associated to the network $\mathcal{W}$.

We discuss this in §8 and compute the spectral coordinates for both Fock-Goncharov and Fenchel-Nielsen type networks.

For the reader's convenience, we first consider the class of Fock-Goncharov type network. For these networks it was shown in [4] (for all $K \geq 2$) that the spectral coordinates are the same as some coordinates introduced earlier by Fock and Goncharov [9]. We give a self-contained re-derivation in the special case $K = 2$ of the fact that Fock-Goncharov networks induce Fock-Goncharov coordinates. We also clarify a few points which might be obscure in [4]; in particular we are more careful about how the story depends on whether we consider connections for the group $SL(2)$ or $PSL(2)$.

We then move on to consider the new class of Fenchel-Nielsen networks. As we explain, the corresponding spectral coordinates are a complexified version of Fenchel-Nielsen (length-twist) coordinates.[4] This is one of our main points: *spectral networks provide a framework which naturally unifies Fock-Goncharov and Fenchel-Nielsen coordinate systems.*

We finish this paper with some physical consequences in §10. As a preview, let us already make some remarks here.

Spectral networks and quadratic differentials

One suggestive way of understanding the results described above comes from the connection between spectral networks and quadratic differentials. Every meromorphic quadratic differential φ_2 on C induces a corresponding spectral network $\mathcal{W}(\varphi_2)$, essentially the critical graph of φ_2. When we consider φ_2 with at least one pole of order ≥ 2, and choose φ_2 generically within this class, the resulting $\mathcal{W}(\varphi_2)$ is a Fock-Goncharov network; this is the basic reason why the previous work [3] focused on Fock-Goncharov networks and the associated Fock-Goncharov coordinate systems.

This motivates the question: what about *non*-generic φ_2? If φ_2 is a Strebel differential — this case is maximally non-generic in a sense — then the corresponding network $\mathcal{W}(\varphi_2)$ is a Fenchel-Nielsen network. (If φ_2 is somewhere intermediate between being fully generic and being a Strebel differential, then we obtain a more general kind of network, called *mixed* in this paper; we do not explore these much, although we expect they can be studied by the methods of this paper.)

Motivations from physics

Another motivation for being interested in Fenchel-Nielsen networks comes from the link between spectral networks and $\mathcal{N} = 2$ supersymmetric field theories. Recall that given a punctured Riemann surface C there is a corresponding $\mathcal{N} = 2$ theory $S[A_1, C]$ as discussed in [16, 3, 2]. The quadratic differentials φ_2 just discussed correspond to points of the Coulomb branch of this theory.

In some approaches to understanding the AGT correspondence [17], complexified Fenchel-Nielsen coordinates on the moduli of $SL(2)$-connections play an important role. For example, in [15] a semiclassical limit of the Nekrasov partition function of the theory $S[A_1, C]$ gets identified with the generating function, in complexified Fenchel-Nielsen coordinates, of the variety of opers inside the moduli space of flat $SL(2)$-connections on C. Fenchel-Nielsen coordinates are also important in the interpretation of the AGT correspondence given in [18].

The result of this paper gives a new way of understanding the role of Fenchel-Nielsen coordinates in the theories $S[A_1, C]$, and thus may shed further light on these approaches. We limit ourselves here to a few optimistic comments, as follows.

[4] Length-twist coordinates were originally defined by Fenchel and Nielsen, in a manuscript recently published as [10]. See also [11, 12]. A complex version of Fenchel-Nielsen coordinates was found in [13, 14, 15].

- First, in this paper the complexified Fenchel-Nielsen coordinates get linked to a particular locus of the Coulomb branch, corresponding to the set of Strebel differentials. This locus is a “real” subspace inside the Coulomb branch: indeed, it is the locus where all of the vector multiplet scalars a^I are real, with respect to a particular choice of electromagnetic frame corresponding to the pants decomposition. It is interesting that this real subspace has played a distinguished role in applications to $\mathcal{N} = 2$ theory in the past. For example, in the computation of the S^4 partition function via localization [19], one naturally considers integrals not over the whole Coulomb branch but rather over this real subspace. Also, it appears that the spectrum of framed BPS states at this real subspace is especially simple: as we describe in §10.2 below, at this locus the UV line defects corresponding to Wilson loops carry just two framed BPS states, exactly matching the naive classical expectation.
- One would like to extend the approaches of [15, 18] to other Lie algebras, e.g. to the case A_{K-1}. The question then arises: *what is the higher rank analogue of Fenchel-Nielsen coordinates?*

  In this paper we find that Fenchel-Nielsen coordinates correspond to the spectral networks which appear at a real locus of the Coulomb branch for $K = 2$. This suggests that one might be able to find higher rank Fenchel-Nielsen coordinates in a similar way, by studying spectral networks appearing at a real locus of the Coulomb branch for $K > 2$.
- The constructions of [18] make use of a correspondence between Fenchel-Nielsen length coordinates ℓ^I and local coordinate functions a^I on the Coulomb branch of the $\mathcal{N} = 2$ theory, i.e. on the Hitchin base. The invariant meaning of this correspondence is a bit mysterious at first glance. After all, ℓ^I and a^I are not the same. Both of them can be viewed as functions on the moduli space of flat connections, but they are different functions, indeed even holomorphic in different complex structures on that hyperkähler space — the ℓ^I are holomorphic in the usual complex structure, while the a^I are holomorphic after rotating to the Higgs bundle complex structure. The correct relation between the two is an *asymptotic* one, of the schematic form

$$\ell^I \sim const \times \exp(const \times a^I/\zeta) \quad \text{as} \quad \zeta \to 0, \tag{1.2}$$

  obtained by applying the WKB approximation to certain 1-parameter families of flat connections. Of course, this relation is noted in [18] too. What we add here is just the observation that this asymptotic relation — and an understanding of its precise range of validity — arises naturally from the point of view of the Fenchel-Nielsen spectral networks; see §10.1 below.

Acknowledgements

We thank Anna Wienhard for a very helpful discussion, and the anonymous referee for many clarifying suggestions, comments and corrections. The research of LH is supported by a Royal Society Dorothy Hodgkin fellowship. The research of AN is supported by NSF grant 1151693. This work was also supported in part by the National Science Foundation under Grant No. PHYS-1066293 and we thank the hospitality of the Aspen Center for Physics.

2 Spectral networks

In this section we start with the definition of spectral network, and then introduce the particular classes of spectral networks we will consider in this paper.

We first describe the class of "Fock-Goncharov networks." Such networks are associated to ideal triangulations of the surface C. They played the starring role in [3]. Second, we introduce a new class of spectral networks which we call "Fenchel-Nielsen networks." These networks are associated to pants decompositions of the surface C rather than triangulations. They have not been considered explicitly before. Third, we briefly consider two more general kinds of network: one obtained by collapsing some double walls in a Fenchel-Nielsen network, which we call "contracted Fenchel-Nielsen", and another which is part Fock-Goncharov and part Fenchel-Nielsen, which we call "mixed".

2.1 Spectral networks

Let C denote an oriented real surface of negative Euler characteristic. C may (but need not) have punctures and/or boundary components.

Let Σ denote a branched double cover of C, which restricts to a trivial cover in a neighborhood of each puncture or boundary component. We often find it convenient to choose a system of branch cuts on C and trivialize the cover Σ on the complement of the cuts, labeling its sheets by an index $i \in \{1, 2\}$.

A *spectral network* $\mathcal{W}$ *subordinate to* Σ is a collection of oriented open paths w on C, which we call *walls*, with the following properties and structure:

- Each wall w begins at a branch point of $\pi : \Sigma \to C$, and ends either at a puncture or at a branch point. A wall ends at a branch point if and only if it overlaps with another wall which is oriented in the opposite direction. We say that the locus where two walls overlap is a "double wall."
- Walls never intersect one another or self-intersect, except that it is possible for two oppositely oriented walls to overlap, as we have just remarked.
- Each wall w carries an ordering of the 2 sheets of the covering Σ over w. If we fix a system of branch cuts and trivialization of Σ, this amounts to saying w locally carries either the label 12 or 21, and the label changes when w crosses a branch cut.
- Exactly three walls w begin at each branch point. If we fix a system of branch cuts and trivialization of Σ, then consecutive walls carry opposite sheet orderings, unless we cross a branch cut in moving from one to the next (or more generally, an odd number of branch cuts); see Figure 1.
- The two constituents in a double wall carry opposite sheet orderings: thus, if we have fixed a labeling of the sheets, then locally one is labeled 12 and the other 21.

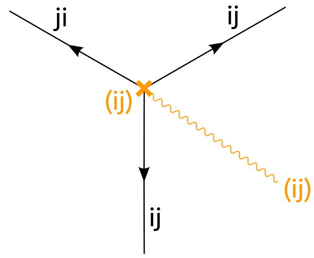

Figure 1: Local configuration of walls near a branch point.

- If there is at least one double wall, then the network comes with an additional discrete datum, the choice of a *resolution*, which is one of the two words "British" or "American". We think of the resolution as telling us how the two constituents of each double wall are infinitesimally displaced from one another; see Figure 2 for the rules.

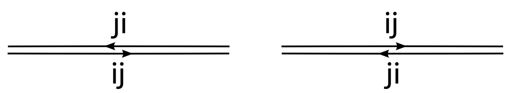

Figure 2: Left: a double wall with American resolution. Right: a double wall with British resolution.

- The closure of each connected component of $C \setminus \mathcal{W}$ must either have one of the topologies shown in Figure 3, or be obtained from one of those topologies by some identifications along the boundary. (In particular, this implies that each puncture has at least one wall ending on it, while boundary components have no walls ending on them.)

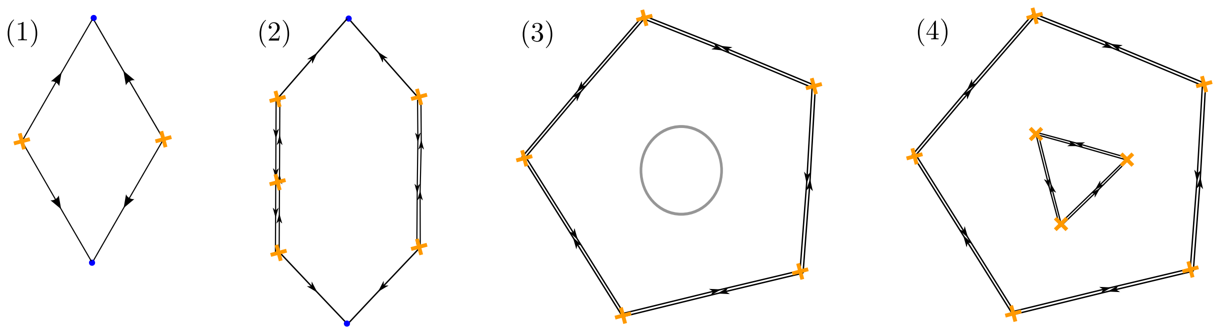

Figure 3: Possible topologies for the connected components of $C \setminus \mathcal{W}$: (1) A generic cell, with two punctures and two branch points as vertices. (2) A degenerate cell, with two punctures and at least three branch points as vertices; each pair of neighboring branch points is connected by a double wall. (3) An annulus bounded by a boundary component on one side and a polygon of double walls on the other. (4) An interior annulus, bounded by a polygon of double walls on each side, with the same resolution on each double wall.

- The spectral network carries a *decoration*, which means a collection of decorations, one for each puncture on C and one for each annulus of $C \setminus \mathcal{W}$:

– A decoration of a puncture $z_l \in C$ is an ordering of the sheets of Σ over z_l, such that the labels of all walls which end on z_l match the decoration at z_l.

– Call a cell of type (3) or (4) from Figure 3 an *annulus in* $C \setminus \mathcal{W}$. Each such annulus A retracts to a circle $c(A) \subset A$. A decoration of A is an assignment of an ordering of the sheets of Σ over A to each orientation o of $c(A)$, such that reversing o also reverses the ordering. The orientation of any wall w on the boundary of A induces an orientation o_w on $c(A)$ (to see this, isotope $c(A)$ to the boundary of A, so that w becomes a subset of $c(A)$); the ordering which the decoration assigns to the orientation o_w must match the label of w.

Let us emphasize that while the punctures and the covering $\Sigma \to C$ are part of the definition of a spectral network, the choice of branch cuts and trivialization of Σ are not: they just give an explicit presentation of Σ, which comes in handy when we want to draw figures and describe examples explicitly.

For later use we remark that any spectral network as defined above has $-2\chi(C)$ branch points. Indeed, we can compute $\chi(C)$ by summing up contributions from the cells. We compute the contribution from a single cell as follows: each edge contributes $-1/2$ (since it will appear on the boundary of two cells), each branch point contributes $+1/3$ (since it will appear on the boundary of three cells), and the interior face contributes $+1$. For example, for a cell of type (2) in Figure 3, we have b branch points and $b+2$ edges, so we get in this way $b/3 - (b-2)/2 + 1 = -b/6$. Similarly for the other cell topologies we always find $-b/6$. Thus summing up over all cells we get $\chi(C) = -\sum b_i/6$. Since $\sum b_i$ is 3 times the total number of branch points on C this gives the desired result.

Finally we define the notion of *equivalence*. Roughly speaking, two spectral networks are equivalent if one can be isotoped into the other. More precisely, given two spectral networks $\mathcal{W}$ and $\mathcal{W}'$ subordinate to covers Σ and Σ', an *equivalence* between $\mathcal{W}$ and $\mathcal{W}'$ is a 1-parameter family of spectral networks $\mathcal{W}_t$ and covers Σ_t, together with an identification of $(\mathcal{W}_0, \Sigma_0)$ with $(\mathcal{W}, \Sigma)$ and $(\mathcal{W}_1, \Sigma_1)$ with $(\mathcal{W}', \Sigma')$. Most of our constructions depend only on a spectral network up to equivalence.

2.2 Fock-Goncharov networks

Suppose that C has at least one puncture and no boundary components. Fix an *ideal triangulation* $\mathcal{T}$ of C, i.e. a triangulation for which the set of vertices is precisely the set of punctures on C.[5] We now construct a network $\mathcal{W}(\mathcal{T})$, the *Fock-Goncharov network* corresponding to $\mathcal{T}$:

1. First, choose one point b inside each triangle of $\mathcal{T}$. We will construct a double cover $\pi : \Sigma \to C$ which is branched exactly at these points. Σ is given explicitly by gluing together two copies of C along a system of branch cuts, with 3 cuts emanating from each branch point b and exiting the 3 sides of the triangle.

2. Next we describe the walls of the network $\mathcal{W}(\mathcal{T})$: for each branch point b, there are three walls, running from b to the three vertices of the triangle in which b sits.

[5] We could allow $\mathcal{T}$ to include some "degenerate" triangles, obtained e.g. by gluing together two vertices or two edges of an ordinary triangle; see [9, 3] for the precise class of triangulations one can allow.

3. Finally, according to the definition of spectral network, we must provide each wall w with an ordering of the two sheets of Σ over w, and we must also decorate each puncture with an ordering of the two sheets near the puncture. Since our construction of Σ equips it with a natural trivialization away from the branch cuts, this amounts concretely to putting labels ij on the walls and punctures. We simply assign the label 12 to every wall and to every puncture.[6]

The conditions in §2.1 are then easy to verify. See Figure 4 for the local picture in each triangle.

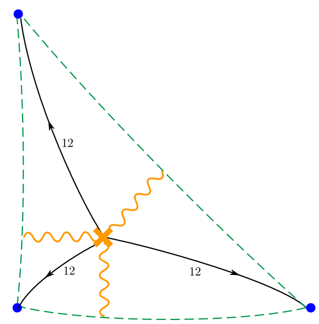

Figure 4: A Fock-Goncharov network $\mathcal{W}(\mathcal{T})$, restricted to a single triangle of $\mathcal{T}$. Walls are drawn as oriented black paths; the orange cross is a branch point; wavy orange lines are branch cuts; dashed green paths are edges of $\mathcal{T}$.

As just described, we build the covering Σ by gluing along a complicated system of branch cuts; this presentation has the advantage of being canonical, but in any particular example, Σ can often be presented by gluing in a simpler way. We will generally take advantage of that freedom when we show explicit examples. Two complete networks are shown in Figure 5.

2.3 Fenchel-Nielsen networks

Now consider a surface C with no punctures, and possibly with boundary components. Fix a pants decomposition $\mathcal{P}$ of C. Given this decomposition we now explain how to construct several different networks, all of which we call *Fenchel-Nielsen networks* associated to $\mathcal{P}$. On each pair of pants we fix the branched cover Σ and spectral network $\mathcal{W}$ to be one of the two shown in Figure 6. We then glue together along the boundaries of the pairs of pants, inserting a circular branch cut around each pants curve. Finally we must specify the decoration: on each annulus in Figure 6 it assigns the sheet ordering 12 to the counterclockwise orientation.[7] This completes the construction of the network.

For instance, Figure 7 depicts a Fenchel-Nielsen network on the four-holed sphere (equivalent to the one obtained from the rules of gluing pants as just formulated).

There is a sense in which a Fenchel-Nielsen network can be considered as a limit of Fock-Goncharov networks. See Figure 8 for an illustration of what we mean. This limiting

[6]Choosing instead 21 everywhere would lead to an equivalent network $\mathcal{W}'(T)$. (Indeed, we define the equivalence between $\mathcal{W}(T)$ and $\mathcal{W}'(T)$ by the identification of $\mathcal{W}(T)$ with $\mathcal{W}'(T)$ that changes all labels.)

[7]Note that this would not have worked without the extra branch cuts around the pants curves.

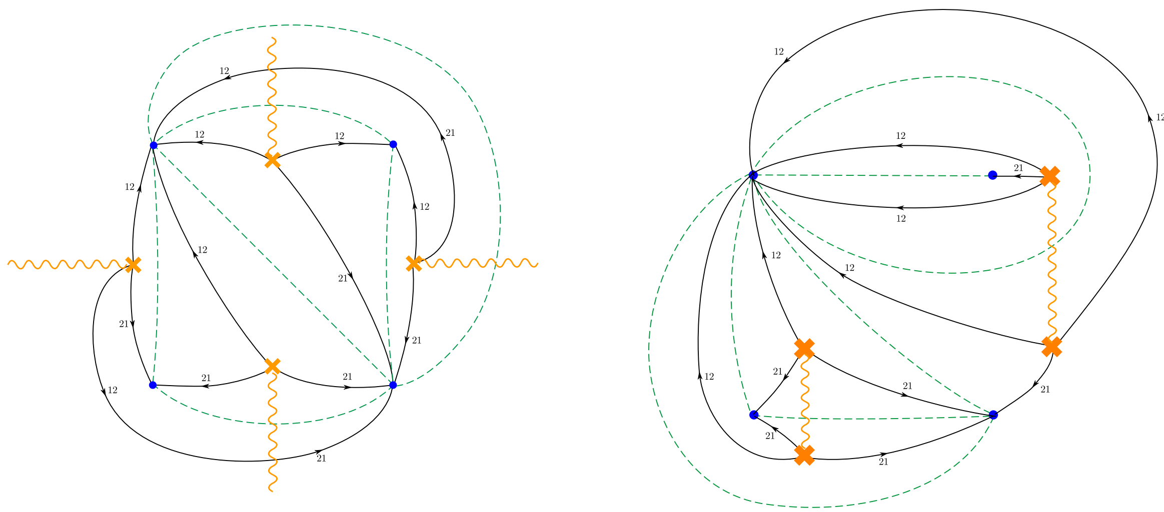

Figure 5: Two examples of Fock-Goncharov networks on the four-punctured sphere (shown here as the plane, with the point at infinity omitted.) The triangulation on the right includes two degenerate triangles. To simplify the figures, here we chose to present the coverings with the minimal possible number of branch cuts; nevertheless one can check directly that the networks shown here are equivalent to the ones we described in the construction of the Fock-Goncharov network.

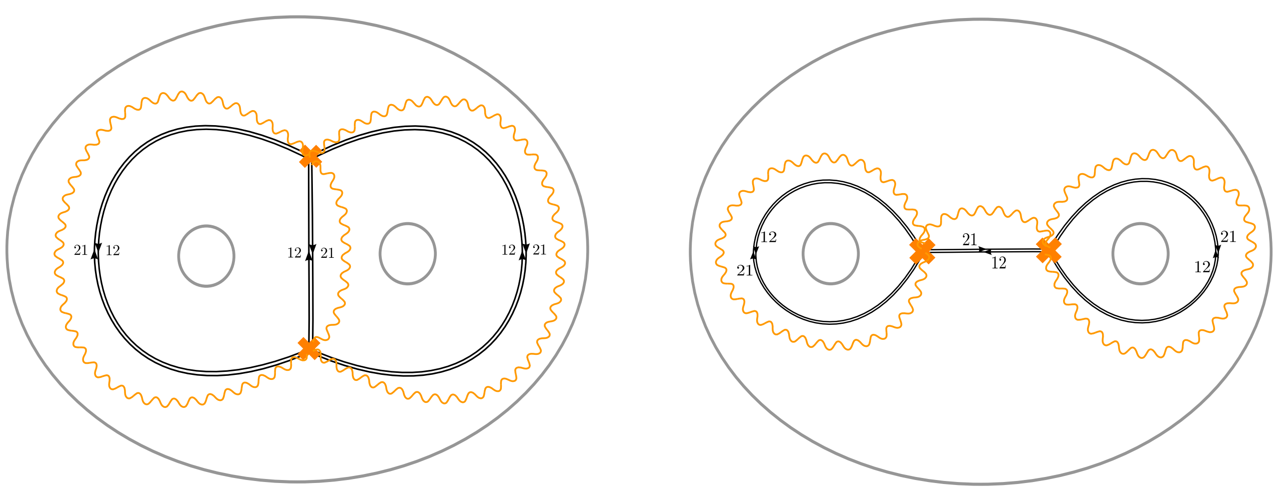

Figure 6: Two examples of Fenchel-Nielsen spectral networks on pairs of pants. The network on the left is "molecule I" and on the right is "molecule II." Each network carries the "British resolution"; to get the "American resolution" one would reverse the orientation of every wall in the network.

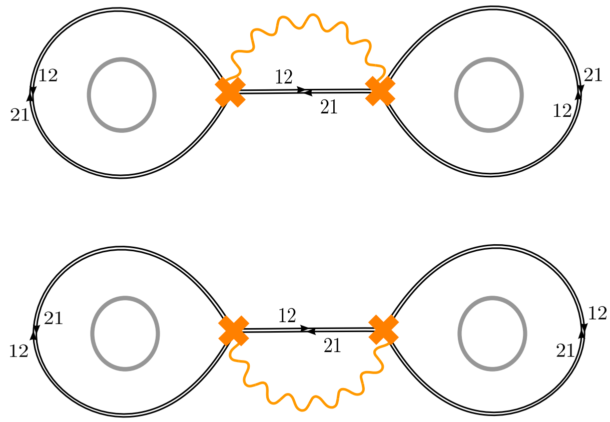

Figure 7: A Fenchel-Nielsen network on the four-holed sphere. This network is built by gluing together two pairs of pants, each containing a copy of molecule II from Figure 6.

procedure has a particularly transparent meaning if we consider the spectral networks as coming from quadratic differentials on C. We explain this in §3 below.

2.4 Contracted Fenchel-Nielsen networks

As we have explained, in Fenchel-Nielsen networks all walls are double walls; however, there are also spectral networks which are not Fenchel-Nielsen networks in which all walls are double walls. See e.g. Figure 9. We refer to such a network as a *contracted* Fenchel-Nielsen network; the reason for the name is that any contracted Fenchel-Nielsen network can be obtained by a degeneration of an ordinary Fenchel-Nielsen network where some annulus shrinks to zero size, in the sense indicated in Figure 10.[8] In fact, as we see in that figure, one may obtain a single contracted Fenchel-Nielsen network by degeneration from several distinct Fenchel-Nielsen networks, associated to different pants decompositions.

2.5 Mixed spectral networks

We call any spectral network that contains both single and double walls a mixed spectral network. An example is given in Figure 11.

3 WKB spectral networks

Let $\bar{C}$ be a closed surface, $\{z_1, \ldots, z_n\} \in \bar{C}$ some points, and $C = \bar{C} \setminus \{z_1, \ldots, z_n\}$. In this section we review from [3] how to construct a canonical spectral network $\mathcal{W}(\varphi_2, \vartheta)$

[8]To see that *every* contracted Fenchel-Nielsen network can be obtained in this way, consider a connected component of the network containing more than two branch points, then look for two which are connected by exactly one double wall; one can define an operation which detaches these two branch points from the rest, creating a new annulus; iterating this operation one eventually reaches an ordinary Fenchel-Nielsen network.

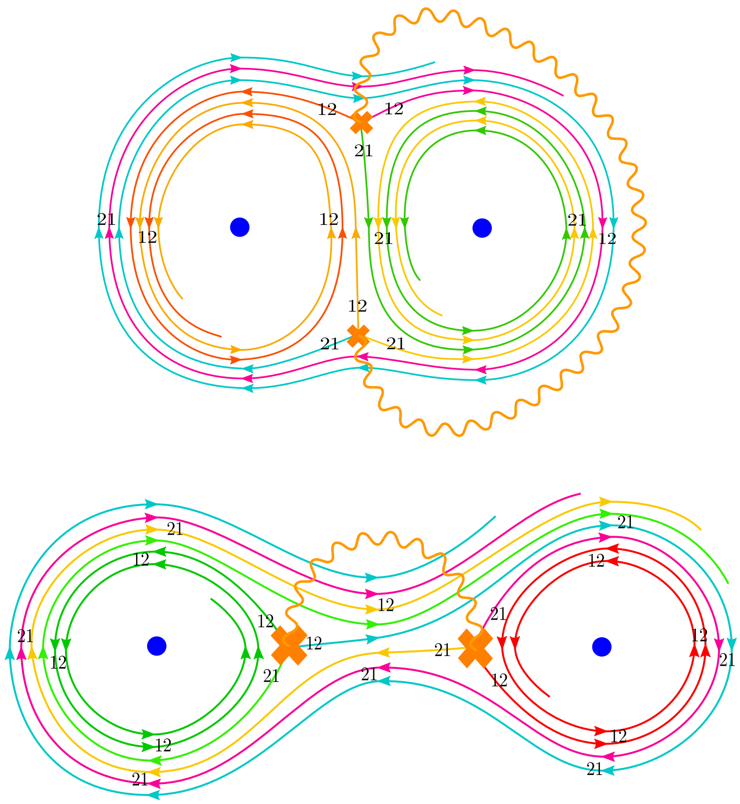

Figure 8: Two spectral networks on the three-punctured sphere (with one puncture at infinity). Each wall spirals many times around and asymptotically approaches some puncture; in the top network, two walls approach each puncture, while in the bottom network, four walls approach the puncture at infinity, and one wall approaches each of the other two punctures. To reduce clutter we show only truncated versions of the walls, and to help distinguish the different walls, they are shown in different colors. These networks are Fock-Goncharov networks, but in the limit where the separation between walls goes to zero, they approach the British resolution of Fenchel-Nielsen molecule I (top) and molecule II (bottom).

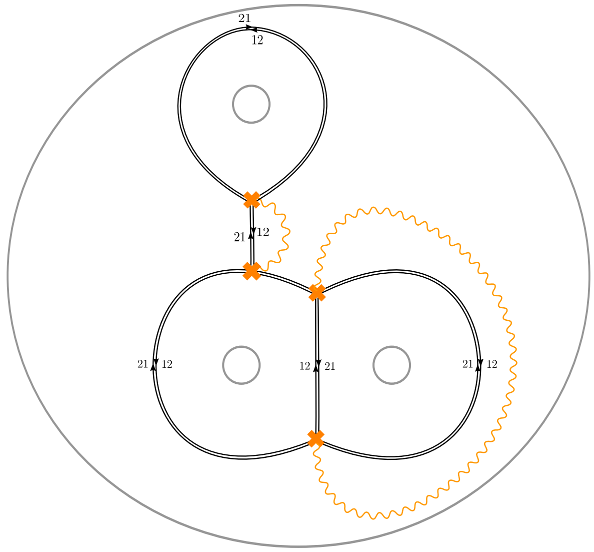

Figure 9: A contracted Fenchel-Nielsen network on the four-holed sphere.

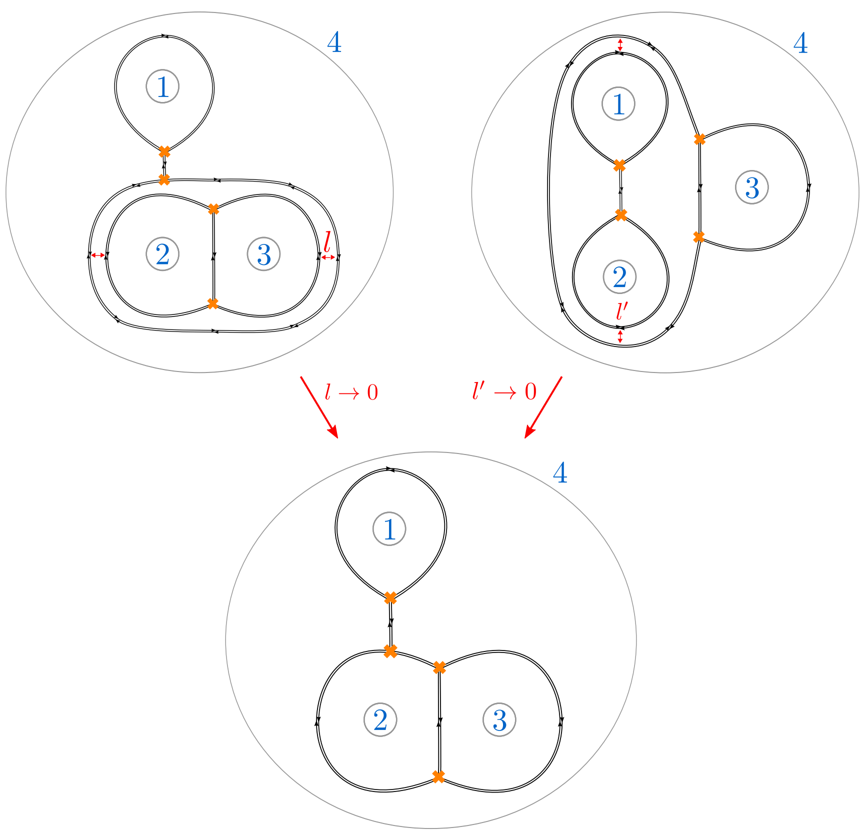

Figure 10: A contracted Fenchel-Nielsen network on the four-holed sphere, which can be obtained in a degeneration limit from two distinct Fenchel-Nielsen networks. These Fenchel-Nielsen networks are associated to two different choices of pants decomposition of the four-holed sphere. (The two branch points referred to in footnote 8 are the ones connecting regions 1 and 2 in the $l \to 0$ limit, and the ones connecting regions 2 and 3 in the $l' \to 0$ limit.)

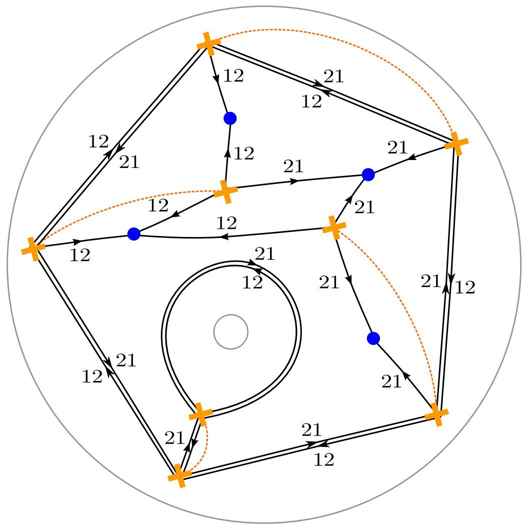

Figure 11: A mixed spectral network on a sphere with four punctures and two holes.

on C, determined by the data of a complex structure on $\bar{C}$, a meromorphic quadratic differential φ_2 on $\bar{C}$ with double poles at the z_l, and a phase $\vartheta \in \mathbb{R}/2\pi\mathbb{Z}$. Spectral networks constructed in this way are known as *WKB spectral networks*.

The class of WKB spectral networks overlaps with all classes of spectral networks introduced above. As we will describe, if (φ_2, ϑ) is chosen generically and φ_2 has at least one double pole, then $\mathcal{W}(\varphi_2, \vartheta)$ is a Fock-Goncharov network. In contrast, if we choose (φ_2, ϑ) in a special way, so that $e^{-2i\vartheta}\varphi_2$ is a *Strebel differential* (i.e. there is a pants decomposition of C such that the period of $\sqrt{\varphi_2}$ around each leg has phase ϑ), then $\mathcal{W}(\varphi_2, \vartheta)$ is a Fenchel-Nielsen network. (To be consistent with our previous definitions, we want to replace each puncture that is surrounded by a polygon consisting of double walls with a boundary.)

The reader who is only interested in understanding how abelianization and nonabelianization work can safely skip this section. However, the construction of WKB spectral networks might help to motivate the definition of spectral network, and will be relevant again in the applications in §10.

In the application to quantum field theories of class $S[A_1]$, the space of meromorphic quadratic differentials φ_2 on C is the Coulomb branch. Fock-Goncharov networks thus appear at generic points of the Coulomb branch, and Fenchel-Nielsen networks appear at distinguished "real" points.

3.1 Foliations

Let φ_2 be a meromorphic quadratic differential on $\bar{C}$, holomorphic away from the z_l. Locally such a differential is of the form

$$\varphi_2 = u(z)(\mathrm{d}z)^2. \tag{3.1}$$

We suppose that φ_2 has only simple zeroes, and second-order poles at the punctures z_l, with residues $-m_l^2 \neq 0$. Such a φ_2 has $-2\chi(C)$ zeroes.

Fixing an angle $\vartheta \in \mathbb{R}/2\pi\mathbb{Z}$, define a (φ_2, ϑ)-*trajectory* to be a real curve on C such that, if v denotes a nonzero tangent vector to the curve,

$$e^{-2\mathrm{i}\vartheta}\varphi_2(v^2) \in \mathbb{R}_+. \tag{3.2}$$

Locally parametrizing such a curve as $z = \gamma(t)$, we can write this condition more concretely as

$$e^{-2\mathrm{i}\vartheta}\, u(\gamma(t)) \left(\frac{\mathrm{d}\gamma(t)}{\mathrm{d}t}\right)^2 \in \mathbb{R}_+. \tag{3.3}$$

The (φ_2, ϑ)-trajectories are leaves of a singular foliation $\mathcal{F}(\varphi_2, \vartheta)$ on C. When $\vartheta = 0$ this is sometimes called the "horizontal foliation" attached to φ_2.

The foliation $\mathcal{F}(\varphi_2, \vartheta)$ has singularities at the zeroes and poles of φ_2. Around a pole z_l the foliation depends on the value of $e^{-\mathrm{i}\vartheta}m_l$, as illustrated in Figure 12. In a neighborhood

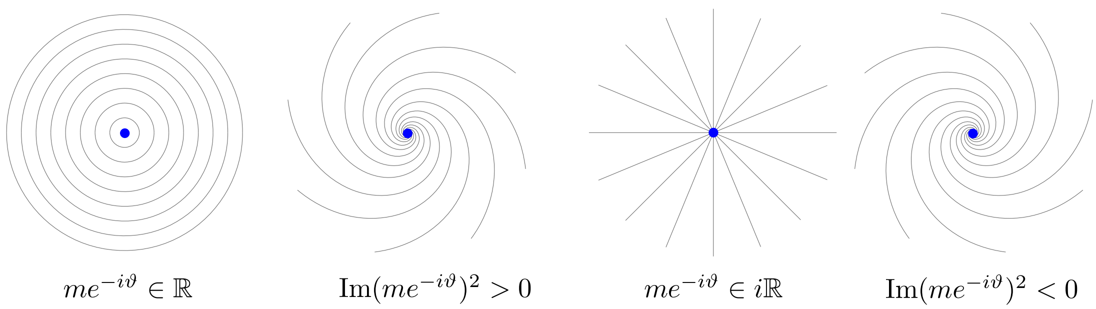

Figure 12: The behavior of the foliation $\mathcal{F}(\varphi_2, \vartheta)$ around a pole of φ_2.

of a zero of φ_2, the foliation $\mathcal{F}(\varphi_2, \vartheta)$ looks like Figure 13. The leaves which terminate at

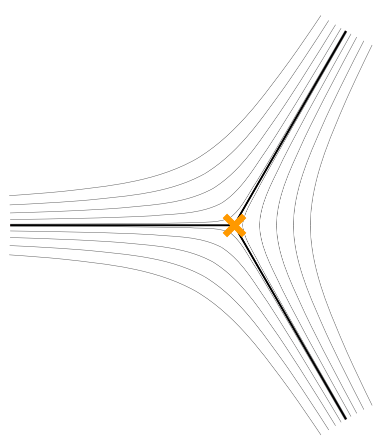

Figure 13: The behavior of the foliation $\mathcal{F}(\varphi_2, \vartheta)$ around a zero of φ_2. Three critical leaves emanate from the zero.

one end on a zero of φ_2 are called "critical." The union of the critical leaves is known as the *critical graph* $CG(\varphi_2, \vartheta)$ of the foliation.

Now we can define a spectral network $\mathcal{W}(\varphi_2, \vartheta)$, as follows. The double covering $\pi : \Sigma \to C$ will be the one given by the square roots of φ_2, i.e.

$$\Sigma = \{(z \in C, \lambda \in T_z^* C) : \lambda^2 = \varphi_2(z)\}, \tag{3.4}$$

with $\pi(z, \lambda) = z$. In local coordinates, writing $\lambda = y\, \mathrm{d}z$, Σ is given by the equation

$$y^2 = u(z). \tag{3.5}$$

Thus the branch points of the covering $\pi : \Sigma \to C$ are the zeroes of φ_2.

The walls of $\mathcal{W}(\varphi_2, \vartheta)$ are roughly the leaves of $CG(\varphi_2, \vartheta)$, but we have to take a bit of care concerning the orientations, as follows. There are two possible behaviors for a leaf of $CG(\varphi_2, \vartheta)$. One possibility is that the leaf has one end on a branch point and the other end on a puncture. In this case the leaf gives a single wall of $\mathcal{W}(\varphi_2, \vartheta)$, oriented *away* from the branch point. The other possibility is that the leaf has both ends on branch points (saddle connection.) In this case the leaf gives a double wall of $\mathcal{W}(\varphi_2, \vartheta)$.[9]

To be consistent with our previous definitions of the various kinds of spectral networks, we replace a puncture with a boundary (defined by a non-critical leaf of the corresponding singular foliation) if the puncture is surrounded by a polygon consisting of double walls.

Next we have to explain how the walls are labeled. Fix a wall w corresponding to a leaf $\gamma(t)$. The two sheets of Σ over w, labeled by the index i, correspond to the two square roots λ_i of φ_2 over w. Given a positively oriented tangent vector v to w, we consider the quantity $q_i = e^{-i\vartheta} \lambda_i(v)$. From (3.3) it follows that q_i is real; it will be positive for one choice of square root (say $i = i_+$) and negative for the other (say $i = i_-$). We label the wall w by the ordered pair $i_- i_+$. [10]

Finally we describe the decorations of the punctures and annuli. First consider a puncture z_l. In a neighborhood of z_l we may label the sheets of Σ by $i = 1, 2$; each square root λ_i of φ_2 has a simple pole near z, with residue $r_i = \pm \mathrm{i} m_l$. Generically, one of the two sheets will have $\mathrm{Re}(e^{-\mathrm{i}\vartheta} r_i) > 0$; the decoration at the puncture z_i is obtained by labeling the sheets with this sheet first. One then checks by a local analysis of (3.3) [3] that the only walls which fall into this puncture are ones whose labeling matches the decoration, as required. Next consider an annulus A of $C \setminus \mathcal{W}(\varphi_2, \vartheta)$. Such an annulus is foliated by closed leaves of $\mathcal{F}(\varphi_2, \vartheta)$. Fix one such leaf and choose an orientation o for it; having done so, we can again consider the quantity $q_i = \lambda_i(v)$ for v a positively oriented tangent vector. q_i is positive for one choice of i, say i_+, and negative for the other, say i_-. Our decoration of the annulus A assigns the ordering $i_- i_+$ to the orientation o. This definition is evidently compatible with the labelings of the walls on the boundary.

[9] By perturbing ϑ slightly to $\vartheta + \epsilon$ this wall would be resolved into two single walls which are close together; in the limit as $\epsilon \to 0^{\pm}$, we may think of these two walls as becoming infinitesimally separated, with the $\pm$ sign determining whether we get the American or the British resolution.

[10] The reason for this choice of labeling is as follows [3]: it guarantees that, when we study certain 1-parameter families of connections $\nabla(\zeta)$ of the form (10.3) below, the corrections $\mathcal{S}_w$ attached to walls of the spectral network will be exponentially *small* as $\zeta \to 0$ — thus these corrections will not affect the asymptotics in that limit.

3.2 Generic differentials and Fock-Goncharov networks

Suppose C has at least one puncture and (φ_2, ϑ) are chosen generically. In this case all leaves of $\mathcal{F}(\varphi_2, \vartheta)$ end at punctures [3]. The corresponding WKB network $\mathcal{W}(\varphi_2, \vartheta)$ is a Fock-Goncharov network. See Figure 14 for an example.

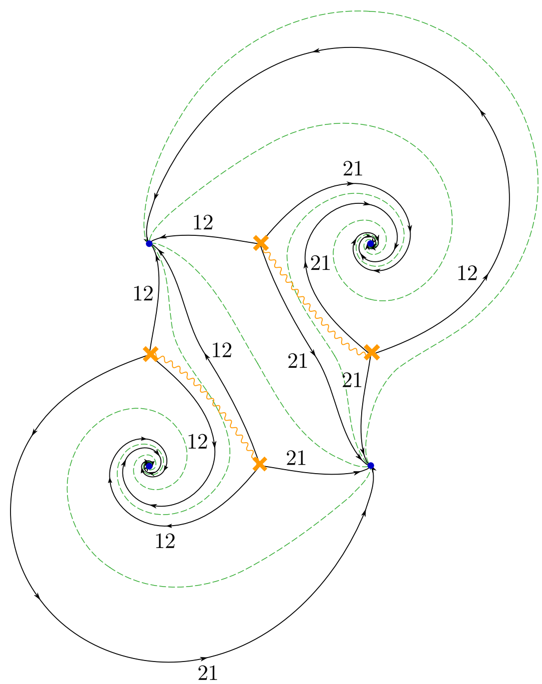

Figure 14: A generic WKB spectral network $\mathcal{W}(\varphi_2, \vartheta)$ on the four-punctured sphere, with $\varphi_2 = \frac{z^4-1}{(z^4+4)^2}\mathrm{d}z^2$ and $\vartheta = \frac{2\pi}{3}$. This network is a Fock-Goncharov network; the dashed green paths are the edges of the corresponding (degenerate) ideal triangulation.

3.3 Strebel differentials and Fenchel-Nielsen networks

Now let us consider the opposite extreme: suppose that the foliation $\mathcal{F}(\varphi_2, \vartheta)$ has *no* leaves ending on punctures, and moreover that all leaves are compact. Concretely this means that all leaves are either closed trajectories or saddle connections. This is equivalent to saying that $e^{-2\mathrm{i}\vartheta}\varphi_2$ is a *Strebel differential*.

Under this condition, each component of the complement $C \setminus \mathcal{W}(\varphi_2, \vartheta)$ is a punctured disc, swept out by closed (φ_2, ϑ)-trajectories. The boundary of each such component is a polygon consisting of one or more saddle connections. The WKB spectral network $\mathcal{W}(\varphi_2, \vartheta)$ contains only double walls. After we replace all punctures with boundaries, each defined by a closed (φ_2, ϑ)-trajectory, it is either a Fenchel-Nielsen spectral network or a contracted Fenchel-Nielsen spectral network.

To each component of the complement $C \setminus \mathcal{W}(\varphi_2, \vartheta)$ we can associate a positive number. For any punctured disc D_j this is the coefficient $m_j e^{-\mathrm{i}\vartheta}$ of the Strebel differential at the puncture, which is equivalent to the (φ_2, ϑ)-length of any closed horizontal trajectory γ in D_j. For any annulus R_k this is the (φ_2, ϑ)-height h_k.

Conversely, given any system of simple closed curves $\{\alpha_k\}_{1\leq k\leq p}$ of a punctured Riemann surface C and arbitrary $h_k > 0$, $1 \leq k \leq p$, and $m_j > 0$, $1 \leq j \leq n$, there is a unique Strebel differential φ_2 with the following properties. The differential φ_2 has n punctured discs which are swept out by closed trajectories around the punctures, that have φ_2-length m_j. Moreover, it has p characteristic annuli with type α_k which have φ_2-height h_k. [20]

For example, a Strebel differential on the three-punctured sphere is of the form

$$\varphi_2 = -\frac{m_\infty^2 z^2 - (m_\infty^2 + m_0^2 - m_1^2)z + m_0^2}{z^2(z-1)^2}\,(\mathrm{d}z)^2, \tag{3.6}$$

where all $m_i \in \mathbb{R}$. This φ_2 has double poles at the punctures $z_i = 0, 1, \infty$, with residues $-m_0^2, -m_1^2, -m_\infty^2$, respectively. The networks $\mathcal{W}(\varphi_2, 0)$ are depicted in Figure 6: we get "molecule I" when $m_\infty < m_0 + m_1$, and "molecule II" when $m_\infty > m_0 + m_1$.

Finally we remark that if we perturb ϑ slightly, each annulus of closed trajectories will be replaced by a region of C where the trajectories are spiraling around a finite number of times. As ϑ is varied across the critical phase ϑ_c where the annulus appears, clockwise spiraling leaves are replaced by anti-clockwise spiraling leaves, or vice versa. See Figure 15 for an example.

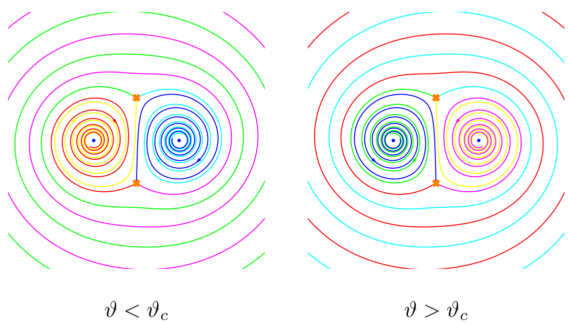

Figure 15: An example of a foliation $\mathcal{F}(\varphi_2, \vartheta)$ near a critical phase ϑ_c where two families of compact leaves appear simultaneously. We label the walls by different colors to make it easier to tell them apart.

3.4 A counterexample

We finish this section by noting that not all spectral networks can arise as WKB spectral networks. A counterexample is given in Figure 16. If this network were a WKB network $\mathcal{W}(\varphi_2, 0)$, then the φ_2-lengths of the critical leaves (measured by integrating $\sqrt{-\varphi_2}$) would obey

$$\ell_1 + \ell_6 = \ell_1 + \ell_2 + \ell_3 + \ell_4,$$
$$\ell_4 + \ell_5 = \ell_2 + \ell_3 + \ell_5 + \ell_6.$$

Clearly, this is impossible for positive real parameters $\ell_1, \ldots, \ell_6$.[11]

[11] This example appears in [21], as an example of a measured foliation which cannot be generated by a quadratic differential. Although the measured foliation is equivalent to one that can be generated by a quadratic differential, this is not the case for the associated spectral network.

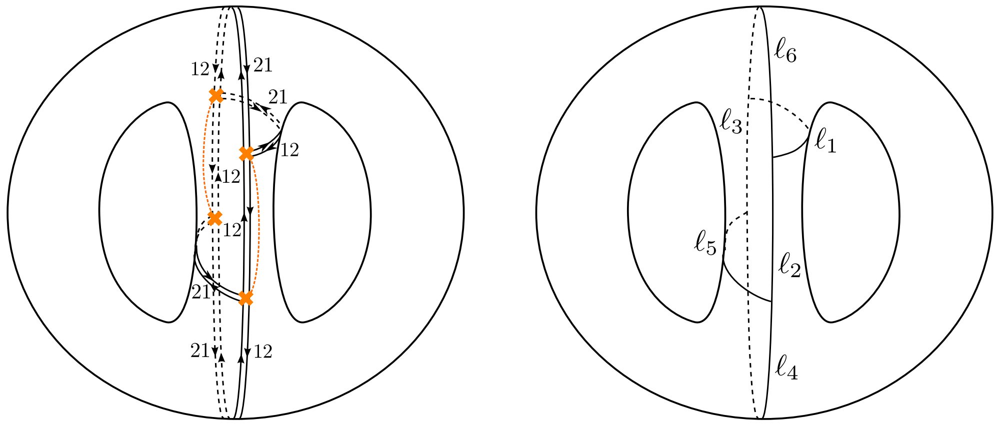

Figure 16: Left: a spectral network on a genus 2 surface that cannot arise as a WKB network $\mathcal{W}(\varphi_2, 0)$ for any φ_2. Right: critical leaves of the corresponding foliation.

4 Abelianization

What is a spectral network good for? Here is one answer: given a Fenchel-Nielsen or Fock-Goncharov spectral network $\mathcal{W}$, and a generic flat $SL(2)$-connection ∇ in a complex rank 2 vector bundle E over C, we can construct a $\mathcal{W}$*-abelianization* of ∇. This is the key to the construction of the "spectral coordinate" systems on the moduli of flat $SL(2)$-connections. In this section we explain this construction.

4.1 $\mathcal{W}$-pairs

A $\mathcal{W}$-abelianization of ∇ is a way of putting ∇ in almost-diagonal form, by locally decomposing E as a sum of two line bundles, $\mathcal{L}_1 \oplus \mathcal{L}_2$, which are preserved by ∇. It is impossible to do this on all of C, but we will come close to that ideal, in the following sense.

Let $\mathcal{W}$ be a spectral network subordinate to the covering $\pi : \Sigma \to C$. Let Σ' denote Σ with the branch points removed. Then:

- A $\mathcal{W}$*-pair* is a tuple $(E, \nabla, \mathcal{L}, \nabla^{\mathrm{ab}}, \iota)$ consisting of:
  - a complex rank 2 vector bundle E over C,
  - a flat $SL(2)$-connection ∇ in E,
  - a complex line bundle $\mathcal{L}$ over Σ',
  - an flat $GL(1)$-connection ∇^{ab} in $\mathcal{L}$,
  - an isomorphism $\iota : E \xrightarrow{\sim} \pi_* \mathcal{L}$ defined over $C \setminus \mathcal{W}$,

  obeying the conditions that
  - the isomorphism ι takes ∇ to $\pi_* \nabla^{\mathrm{ab}}$,
  - ι jumps by a map $\mathcal{S}_w = 1 + e_w \in \mathrm{End}(\pi_* \mathcal{L})$ at each single wall $w \subset \mathcal{W}$, where $e_w : \mathcal{L}_i \to \mathcal{L}_j$ if w carries the label ij. (Here by $\mathcal{L}_i$ we mean the summand of $\pi_* \mathcal{L}$ associated to sheet i. Relative to diagonal local trivializations of $\pi_* \mathcal{L}$, this

condition says $\mathcal{S}_w$ is upper or lower triangular.) ι jumps by a map $\mathcal{S}_{w'}\mathcal{S}_w$ at each double wall $w'w$.

- Given a flat $SL(2)$-connection ∇ in a complex rank 2 bundle E over C, a *$\mathcal{W}$-abelianization* of ∇ is any extension of (E, ∇) to a $\mathcal{W}$-pair $(E, \nabla, \mathcal{L}, \nabla^{\mathrm{ab}}, \iota)$.
- Given a flat $GL(1)$-connection ∇^{ab} in a complex line bundle $\mathcal{L}$ over Σ', a *$\mathcal{W}$-nonabelianization* of ∇^{ab} is any extension of $(\mathcal{L}, \nabla^{\mathrm{ab}})$ to a $\mathcal{W}$-pair $(E, \nabla, \mathcal{L}, \nabla^{\mathrm{ab}}, \iota)$.

We say $(E, \nabla, \mathcal{L}, \nabla^{\mathrm{ab}}, \iota) \sim (E', \nabla', \mathcal{L}', \nabla'^{\mathrm{ab}}, \iota')$, and call these two $\mathcal{W}$-pairs *equivalent*, if there exist maps $\varphi : \mathcal{L} \to \mathcal{L}'$ and $\psi : E \to E'$ which take ι into ι', ∇^{ab} into ∇'^{ab}, and ∇ into ∇'. In particular, in this case we have equivalences $(\mathcal{L}, \nabla^{\mathrm{ab}}) \sim (\mathcal{L}', \nabla'^{\mathrm{ab}})$ and $(E, \nabla) \sim (E', \nabla')$.

Since the covering $\Sigma \to C$ has at least one branch point, every complex line bundle over Σ' is topologically trivial. Thus, in particular, every $\mathcal{W}$-pair is equivalent to one where $\mathcal{L}$ is taken to be the trivial bundle, so we could have taken $\mathcal{L}$ to be trivial from the start; nevertheless this requirement is a bit unnatural from our point of view, and we prefer to emphasize that $\mathcal{L}$ need not be *canonically* trivial.

4.2 Equivariant $GL(1)$-connections

In this section we will show that the connections ∇^{ab} which arise in $\mathcal{W}$-pairs automatically carry some extra structure: they are *equivariant*, and as a consequence of this, they are also *almost-flat* (both terms to be defined below.)

Suppose given a $\mathcal{W}$-pair $(E, \nabla, \mathcal{L}, \nabla^{\mathrm{ab}}, \iota)$. The fact that ∇ is an $SL(2)$-connection means that the underlying bundle E carries a ∇-invariant, nonvanishing volume form $\varepsilon_E \in \wedge^2(E)$. Introduce the covering involution $\sigma : \Sigma \to \Sigma$. We have a ∇^{ab}-invariant nondegenerate pairing

$$\mu : \mathcal{L} \otimes \sigma^* \mathcal{L} \to \mathbb{C} \tag{4.1}$$

given by[12]

$$\mu(s, s') = (\iota^{-1}(s) \wedge \iota^{-1}(s'))/\varepsilon_E. \tag{4.2}$$

The triangular property of the jumps $\mathcal{S}_w$ shows that μ extends even over $\pi^{-1}(\mathcal{W})$. In particular, μ gives a ∇^{ab}-invariant isomorphism $\mathcal{L} \simeq \sigma^* \mathcal{L}^*$.

The antisymmetry of the wedge product means μ has a slightly tricky "antisymmetry" property: if we consider

$$\sigma^* \mu : \sigma^* \mathcal{L} \otimes \mathcal{L} \to \mathbb{C} \tag{4.3}$$

using $\sigma^* \sigma^* \mathcal{L} = \mathcal{L}$, and let $\tau : \sigma^* \mathcal{L} \otimes \mathcal{L} \to \mathcal{L} \otimes \sigma^* \mathcal{L}$ be the operation of reversing factors, we have

$$\sigma^* \mu = -\mu \circ \tau. \tag{4.4}$$

We call a connection ∇^{ab} in a line bundle $\mathcal{L}$ equipped with such a pairing *equivariant*.

The equivariance of ∇^{ab} has an important consequence: it implies that the holonomy of ∇^{ab} around a small loop on Σ' encircling a branch point is always -1. To see this,

[12] Here we abuse notation slightly: ι refers to the induced map $\iota : \pi^* E \to \pi^* \pi_* \mathcal{L} \cong \mathcal{L} \oplus \sigma^* \mathcal{L}$ on $\Sigma \backslash \pi^{-1}(\mathcal{W})$.

fix a basepoint z near the branch point. At this point the fiber of $\pi_* \mathcal{L}$ is canonically decomposed into two lines, labeled by the two preimages of z in Σ'. The holonomy of ∇^{ab} around the loop exchanges these two lines; so with respect to a basis (s_1, s_2) respecting this decomposition, it would be represented by an antidiagonal matrix. Moreover the equivariance implies that this holonomy has determinant 1. Combining these facts, the holonomy of $\pi_* \nabla^{\mathrm{ab}}$ around the branch point can be represented by a matrix of the shape

$$\begin{pmatrix} 0 & D \\ -D^{-1} & 0 \end{pmatrix}. \tag{4.5}$$

The holonomy of $\pi_* \nabla^{\mathrm{ab}}$ around a path going twice around the branch point on C is thus

$$\begin{pmatrix} 0 & D \\ -D^{-1} & 0 \end{pmatrix}^2 = \begin{pmatrix} -1 & 0 \\ 0 & -1 \end{pmatrix} \tag{4.6}$$

This says that the holonomy of ∇^{ab} around each branch point on Σ is -1, as desired. We refer to a connection ∇^{ab} with this property as an *almost-flat* connection over Σ.

4.3 $\mathcal{W}$-pairs with boundary and gluing

If C has boundary, it is sometimes useful to consider connections and $\mathcal{W}$-pairs with a bit of extra structure. We fix a marked point on each boundary component of C. Then, a *$\mathcal{W}$-pair with boundary* consists of

- A $\mathcal{W}$-pair $(E, \nabla, \mathcal{L}, \nabla^{\mathrm{ab}}, \iota)$ as in §4.1,
- a trivialization of E_z for each marked point z,
- a trivialization of $\mathcal{L}_{z_i}$ for each preimage $z_i \in \pi^{-1}(z)$ for a marked point z,
- a trivialization of the covering Σ over each marked point z,

such that ι maps the trivialization of E_z to the trivialization of $\pi_* \mathcal{L}_z$ induced from those of $\mathcal{L}_{z_i}$ and Σ.

Given two surfaces C, C' with boundary we can glue along a boundary component, in such a way that the marked points are identified. Now suppose that we have a $\mathcal{W}$-pair with boundary on each of C and C', and that the monodromies around the glued component are the same (when written relative to the given trivializations at the marked points). Then using the trivializations we can glue the two $\mathcal{W}$-pairs to obtain a $\mathcal{W}$-pair over the glued surface.

5 Constructing abelianizations

5.1 A preliminary observation

We begin with an observation which will be useful for the construction of $\mathcal{W}$-pairs in the next few sections. Suppose that in the definition of $\mathcal{W}$-pair we require only that ∇^{ab} is defined on $\Sigma' \setminus \pi^{-1}(\mathcal{W})$. In fact this leads to an equivalent definition: ∇^{ab} automatically extends from $\Sigma' \setminus \pi^{-1}(\mathcal{W})$ to Σ'.

To see this, consider a single wall w carrying the label (say) 21. Choosing a local trivialization of $\mathcal{L}$ in some neighborhood of the interior of $\pi^{-1}(w)$, $\pi_* \mathcal{L}$ also becomes trivial in this neighborhood. Then ι amounts to two bases (s_1, s_2) and (s_1', s_2') for E in a neighborhood of w, related by an upper-triangular transformation,

$$s_1' = s_1, \qquad s_2' = s_2 + \alpha s_1 \tag{5.1}$$

for some function α. These bases diagonalize the connection ∇, so that we have $\nabla s_i = d_i s_i$ on one side of w (for some closed 1-forms d_i) and on the other side $\nabla s_i' = d_i' s_i'$. What we would like to show is that $d_i' = d_i$; this would say that $\pi_* \nabla^{\mathrm{ab}}$ extends over w, or in other words, ∇^{ab} extends over $\pi^{-1}(w)$. But this is now a straightforward computation. First, since $s_1' = s_1$ it follows immediately that $d_1' = d_1$. Now

$$\nabla s_2' = \nabla(s_2 + \alpha s_1) = \nabla s_2 + (\mathrm{d}\alpha) s_1 + \alpha \nabla s_1 \tag{5.2}$$

and

$$\nabla s_2' = d_2' s_2' = d_2'(s_2 + \alpha s_1). \tag{5.3}$$

Comparing these two gives $d_2' = d_2$, as desired (and $\mathrm{d}\alpha = (d_2 - d_1)\alpha$.)

5.2 Fock-Goncharov spectral networks

Suppose we are given a Fock-Goncharov network $\mathcal{W}$ and a flat $SL(2)$-connection ∇ on C. How do we $\mathcal{W}$-abelianize ∇?

Given a flat $SL(2)$-connection ∇ and a puncture z_l on C, let a *framing* of ∇ at z_l be a choice of a ∇-invariant line subbundle ℓ_l of E, in a neighborhood of z_l. We define a *$\mathcal{W}$-framed connection* to be a flat $SL(2)$-connection ∇ plus a choice of a framing at each puncture, subject to an additional condition: if two punctures z_i, z_j can be connected by a path $\mathcal{P}$ which does not meet $\mathcal{W}$, and we use the parallel transport along $\mathcal{P}$ to transport ℓ_i and ℓ_j to a common point $z \in C$, then at this point we get $\ell_i(z) \neq \ell_j(z)$. This condition is automatically satisfied for a generic ∇. Moreover, for generic ∇, there are exactly 2^n possible $\mathcal{W}$-framings, where n is the number of punctures; indeed the monodromy around each puncture has two distinct eigenspaces, and we are just choosing one of them.

In the rest of this section we will show: *$\mathcal{W}$-abelianizations of ∇ up to equivalence are canonically in 1-1 correspondence with $\mathcal{W}$-framings of ∇.*

Let $\mathcal{L}$ be the trivial bundle over Σ. Our $\mathcal{W}$-abelianizations of ∇ will be determined by giving an isomorphism $\iota : E \simeq \pi_* \mathcal{L}$ over $C \setminus \mathcal{W}$. $C \setminus \mathcal{W}$ consists of "cells" with the topology of component (1) in Figure 3; let c denote one such cell.

Suppose we trivialize the covering Σ over c.[13] Giving ι over c is then equivalent to giving $\iota^{-1} : \mathcal{O} \oplus \mathcal{O} \to E$, i.e. a basis (s_1, s_2) of E over c. How will we get this basis? On the boundary of c we have two punctures, each carrying a decoration. Moreover, our rules for spectral networks imply that the two decorations are opposite: thus one puncture is

[13]We emphasize that this is only a *local* trivialization; we can always do this since c is simply connected. Thus in what follows we will not have to worry about branch cuts.

labeled 21 (call this puncture z_1) and the other 12 (call this puncture z_2). Each puncture has a framing; call these ℓ_1 and ℓ_2. By parallel transporting the framings ℓ_1 and ℓ_2 along a path in c to a general $z \in c$, we obtain lines $\ell_1(z)$ and $\ell_2(z)$ in E_z. Our basis (s_1, s_2) is obtained by choosing $s_1(z) \in \ell_1(z)$ and $s_2(z) \in \ell_2(z)$. Crucially, for any such choice, ∇ is diagonal relative to the basis (s_1, s_2); thus ι indeed identifies ∇ with the pushforward of a connection ∇^{ab} in the line bundle $\mathcal{L}$.

Note that this construction would have failed if $\ell_1(z) = \ell_2(z)$, since in that case $s_1(z)$ and $s_2(z)$ are not linearly independent, so they do not form a basis of E_z. This is why we required that $\ell_1(z) \neq \ell_2(z)$ in the definition of $\mathcal{W}$-framed connection.

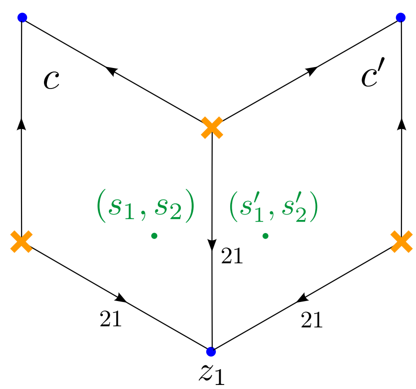

Figure 17: Bases (s_1, s_2) and (s_1', s_2') attached to the two sides of a wall that separates the cells c and c'.

Now let us consider the change-of-basis matrix $\mathcal{S}_w$. Consider the two bases (s_1, s_2) and (s_1', s_2') attached to the two sides of the wall in Figure 17. Because the two cells c, c' have the vertex z_1 in common, we will have $\ell_1 = \ell_1'$, so s_1 and s_1' can differ at most by scalar multiple. This implies that the transformation $\mathcal{S}_w$ taking (s_1, s_2) to (s_1', s_2') has the form

$$\mathcal{S}_w = \begin{pmatrix} * & * \\ 0 & * \end{pmatrix}$$

relative to the basis (s_1, s_2). By a diagonal "gauge transformation" of the form

$$(s_1'(z), s_2'(z)) \mapsto (\lambda_1(z) s_1'(z), \lambda_2(z) s_2'(z)), \tag{5.4}$$

where λ_1 and λ_2 are functions on c', we can thus arrange that

$$\mathcal{S}_w = \begin{pmatrix} 1 & * \\ 0 & 1 \end{pmatrix} \tag{5.5}$$

relative to the basis (s_1, s_2). This is the desired form for the jump of ι according to the definition of $\mathcal{W}$-abelianization.

We have now described a canonical $\mathcal{W}$-abelianization for any ∇ equipped with a $\mathcal{W}$-framing. It only remains to show that in this way we obtain *all* $\mathcal{W}$-abelianizations of ∇. So, suppose we have *any* $\mathcal{W}$-abelianization of the connection ∇. Consider a neighborhood of a puncture z_1 as shown in Figure 18. In each cell, the $\mathcal{W}$-abelianization amounts to a

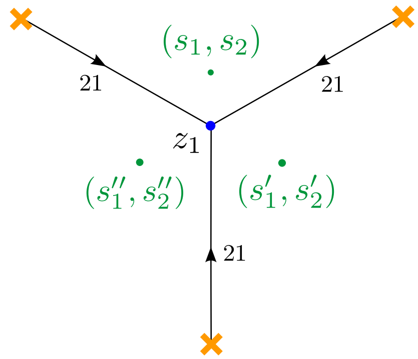

Figure 18: Neighborhood of a puncture with bases.

pair of sections $s_1(z)$, $s_2(z)$, with respect to which ∇ is diagonal. The constraint that $\mathcal{S}_w$ is of the form (5.5) says that $\mathcal{S}_w$ preserves s_1, i.e. along the wall w we have $s_1(z) = s_1'(z)$. Continuing around the wall we see that s_1, s_1', s_1'' are the restrictions of a single section $\hat{s}_1(z)$ defined in a whole punctured neighborhood of the puncture z_1, such that $\nabla \hat{s}_1(z)$ is a multiple of $\hat{s}_1(z)$. In particular, $\hat{s}_1(z)$ is an eigenvector of the monodromy of ∇ around the puncture.

Applying this condition to every puncture is almost enough to determine the $\mathcal{W}$-abelianization. Let us consider the choices remaining. First, there is the choice of *which* eigenvector to take at each puncture. This choice is equivalent to the choice of a $\mathcal{W}$-framing. Second, there is the freedom to make an overall rescaling $(s_1(z), s_2(z)) \to (\lambda_1(z)s_1(z), \lambda_2(z)s_2(z))$ in each cell (matching up along the walls). Such a change only changes the $\mathcal{W}$-abelianization by equivalence. So altogether we have found that $\mathcal{W}$-abelianizations are in 1-1 correspondence with $\mathcal{W}$-framings, as desired.

5.3 Fenchel-Nielsen spectral networks

Next suppose we are given a Fenchel-Nielsen spectral network $\mathcal{W}$ and a flat $SL(2)$-connection ∇ over C.

As for Fock-Goncharov networks, we will need to enrich ∇ by some extra data in order to get a canonical $\mathcal{W}$-abelianization, as follows. The complement $C' = C \setminus \mathcal{W}$ consists of various connected components A, each with the topology of an annulus. There are two ways of going around the annulus; define a *framing* of ∇ on A to be a 1-dimensional eigenspace of the monodromy in each direction (so if we label the two directions $\pm$, we give an eigenspace ℓ_+ of the monodromy M_+ and an eigenspace ℓ_- of the monodromy $M_- = M_+^{-1}$.) We require that $\ell_+ \neq \ell_-$, and also that each of $\ell_\pm$ for any annulus is distinct from each of $\ell_\pm$ for any adjacent annulus.[14] Note that a framing of ∇ on A exists only if $M_\pm$ are diagonalizable. Finally, we define a $\mathcal{W}$-framed connection to be a flat $SL(2)$-connection ∇ plus a framing of ∇ on each annulus A.

[14]This last constraint would follow from the requirement that ∇ is indecomposable when restricted to any pair of pants. Indeed, suppose that the monodromies around two adjacent annuli A and A' have a common eigenline ℓ, and consider a pair of pants that has A, A' as two of its boundary components; the monodromy around the third boundary of this pair of pants will also have eigenline ℓ.

We can now proceed much as we did for the Fock-Goncharov networks. Fix an annulus A. For any $z \in A$, the framing of ∇ on A gives two lines $\ell_+(z) \subset E_z$ and $\ell_-(z) \subset E_z$. Choose a section $s_+(z)$ valued in $\ell_+(z)$ and a section $s_-(z)$ valued in $\ell_-(z)$. We want to use this pair of sections to build an isomorphism $\iota : E \to \pi_* \mathcal{L}$, where $\mathcal{L}$ denotes the trivial bundle over Σ. Concretely, the covering Σ is trivializable over A (no branch cut crosses the annulus from edge to edge), so we may choose a trivialization; after so doing, what we need to do is to choose which of $s_\pm$ will be s_1 and which will be s_2. This extra information is provided by the decoration of $\mathcal{W}$ on A: if the labeling attached to the $+$ direction is ij, then we take $s_i = s_+$ and $s_j = s_-$.

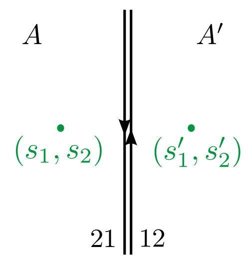

Figure 19: Bases of sections on either side of a double wall that separates two annuli A and A'. (Only a piece of each annulus is shown here; for a sample global picture see Figure 7.)

Now we need to arrange that the change-of-basis matrices $\mathcal{S}_w$ attached to the walls $w \subset \mathcal{W}$ are of the required triangular form. Consider the double wall shown in Figure 19, separating annuli A, A'. What we require is that the matrix taking (s_1, s_2) to (s_1', s_2') is of the form

$$\begin{pmatrix} 1 & * \\ 0 & 1 \end{pmatrix} \begin{pmatrix} 1 & 0 \\ * & 1 \end{pmatrix}. \tag{5.6}$$

This just says that this matrix has determinant 1 and lower left entry 1. Since s_1' and s_2 are not proportional, and s_2' and s_1 are not proportional, we know that neither of the diagonal entries vanishes; thus we can arrange the desired form by a rescaling of the form $(s_1', s_2') \to (\lambda_1(z) s_1', \lambda_2(z) s_2')$.

Finally, we observe that in this way we obtain *all* $\mathcal{W}$-abelianizations of ∇. Indeed, if we have an abelianization of ∇ on an annulus, then the two lines $\iota^{-1}(\mathcal{L}_1)$ and $\iota^{-1}(\mathcal{L}_2)$ must be eigenlines of the monodromy of ∇ around the annulus. The only freedom is the choice of which of these lines is which eigenline, i.e. the choice of framing. Thus $\mathcal{W}$-abelianizations of ∇ are in 1-1 correspondence with $\mathcal{W}$-framings of ∇.

5.4 Fenchel-Nielsen with boundary

Finally we consider a small extension of the above. Suppose that C is a surface with boundary, carrying a Fenchel-Nielsen network $\mathcal{W}$, and a flat $SL(2)$-connection ∇ in a bundle E. Suppose moreover that we fix a marked point z_a on each boundary component, along with a trivialization of E_{z_a}, with respect to which the monodromy is diagonal. In this case our construction of a $\mathcal{W}$-pair in §5.3 is easily extended to construct a $\mathcal{W}$-pair with boundary, in the sense of §4.3.

Suppose we are given two surfaces C, C' with boundary and a flat $SL(2)$-connection on each of C and C' with trivialization at a marked point. If the monodromies around the glued component are the same (when written relative to the given trivializations at the marked points), then we can either first $\mathcal{W}$-abelianize and then glue the resulting $\mathcal{W}$-pairs (as in §4.3), or first glue the two flat $SL(2)$-connections and then $\mathcal{W}$-abelianize. Since the monodromy of the $SL(2)$-connection is diagonal along the boundary component, it is clear that the two actions commute.

5.5 Mixed spectral networks

In the last two sections we have described the process of $\mathcal{W}$-abelianization when $\mathcal{W}$ is a Fock-Goncharov or a Fenchel-Nielsen network. More generally we could take $\mathcal{W}$ to be a mixed spectral network. Such networks lie somewhere between the two extremes just considered. We expect that all of our constructions have analogues when $\mathcal{W}$ is mixed; indeed, all of our constructions were *local*, involving just a particular cell or a particular (single or double) wall. Each cell of $C \setminus \mathcal{W}$ has one of the two topologies we have just dealt with above, so we can determine the abelianization on each cell using the same recipes we used above. Moreover, by appropriate rescalings of the sections (s_1, s_2) on each cell, we will be able to arrange the desired form for the change-of-basis matrices $\mathcal{S}_w$ at each wall, just as we did above.

6 The integrated version

Instead of working directly with flat connections, it will be convenient in the rest of the paper to work with the corresponding integrated objects, namely the parallel transport maps. While this change of emphasis is not strictly necessary, the integrated point of view is very convenient for practical computations, as we will see in the examples of §9 below.

In this section we spell out the details of this integrated version of the story. Thus we will replace flat $SL(2)$-connections on C by $SL(2)$-representations of a certain groupoid $\mathcal{G}_C$ of paths on C, defined below. For the $GL(1)$-connections over Σ we have to do something slightly more complicated, to capture the extra condition that the $GL(1)$-connections we use are equivariant (as we saw in §4.2). Thus we will define below a notion of *equivariant* $GL(1)$*-representation* of a groupoid $\mathcal{G}_{\Sigma'}$ of paths on Σ'. Finally, we will define a notion of *representation* $\mathcal{W}$*-pair* which is the integrated counterpart of an ordinary $\mathcal{W}$-pair.

Path groupoids

First we define the path groupoid $\mathcal{G}_C$. We fix a set $\mathcal{P}_C$ of *basepoints* on C, as follows. For each single wall w we fix two basepoints, which lie very close to one another, one on each side of w. For a double wall we fix three basepoints, one on each side of the wall and one between the two lanes. Finally, we fix one basepoint along each boundary component of C. See Figure 20 for an example.

$\mathcal{G}_C$ is the groupoid whose objects are the points of $\mathcal{P}_C$, and whose morphisms are homotopy classes of paths $\wp$ which begin and end at points of $\mathcal{P}_C$.

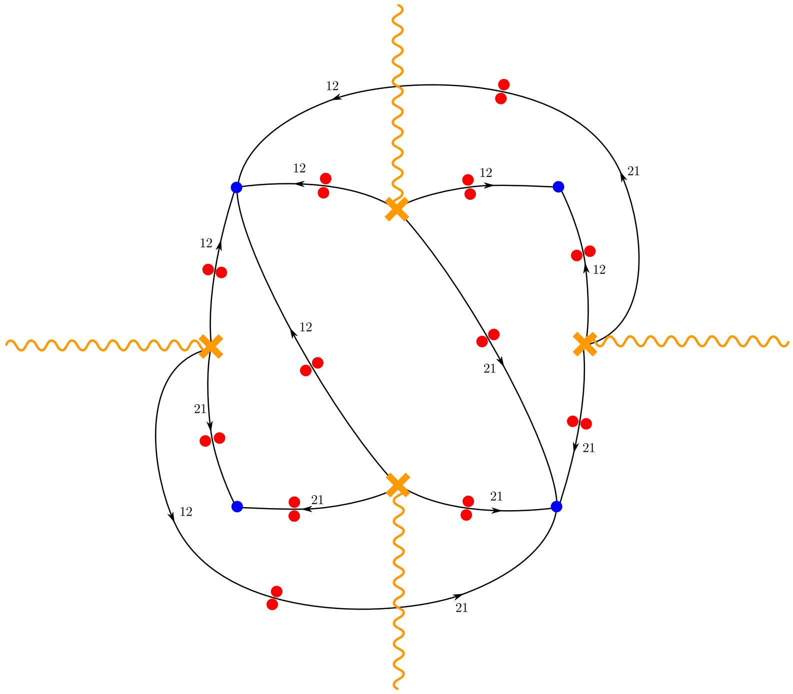

Figure 20: Example of a spectral network with basepoints.

Next we define the path groupoid $\mathcal{G}_{\Sigma'}$ on the double cover. Let $\mathcal{P}_{\Sigma'} = \pi^{-1}(\mathcal{P}_C)$: thus for each $z \in \mathcal{P}_C$ we have two elements $z^{(i)} \in \mathcal{P}_{\Sigma'}$. The objects in $\mathcal{G}_{\Sigma'}$ are just the points of $\mathcal{P}_{\Sigma'}$. The morphisms in $\mathcal{G}_{\Sigma'}$ are homotopy classes of paths on Σ' which begin and end at points of $\mathcal{P}_{\Sigma'}$.

$SL(2)$-representations

By an $SL(2)$-representation ρ of $\mathcal{G}_C$, we mean

- a 2-dimensional vector space E_z for each $z \in \mathcal{P}_C$, together with a nonzero element $\varepsilon_z \in \wedge^2(E_z)$,
- an element $\rho(\wp) : E_{i(\wp)} \to E_{f(\wp)}$ for each morphism $\wp$ of $\mathcal{G}_C$, with initial point $i(\wp)$ and final point $f(\wp)$; ρ should be compatible with composition, and each $\rho(\wp)$ should be compatible with ε in the obvious sense, i.e. have "determinant 1".

An *equivalence* between $SL(2)$-representations ρ, ρ' is a collection of isomorphisms

$$g_z : E_z \to E'_z \tag{6.1}$$

such that for any $\wp \in \mathcal{G}_C$

$$\rho'(\wp) = g_{f(\wp)}\rho(\wp)g^{-1}_{i(\wp)} \tag{6.2}$$

and such that $g_z(\varepsilon_z) = \varepsilon'_z$. Thus $SL(2)$-representations of $\mathcal{G}_C$ form a category.

There is an equivalence between the category of $SL(2)$-representations of $\mathcal{G}_C$ and the category of flat $SL(2)$-connections over C. For completeness we briefly explain how this goes. One direction of the equivalence is easy to describe: given a flat $SL(2)$-connection ∇ in a bundle E over C, define an $SL(2)$-representation ρ of $\mathcal{G}_c$ by the rule that E_z is the fiber of E over z, and $\rho(\mathcal{P})$ is the parallel transport of ∇ along $\mathcal{P}$. For the other direction, we consider the based path space $\tilde{C}$, consisting of homotopy classes of paths on C which begin at points of $\mathcal{P}_C$ and end anywhere. $\tilde{C}$ has one connected component $\tilde{C}_z$ for each $z \in \mathcal{P}_C$. One can recover C from $\tilde{C}$ by dividing out an equivalence relation: two paths p, p' are equivalent if they differ by concatenation with some path $\wp \in \mathcal{G}_C$, $p = p'\wp$.[15] Now suppose given an $SL(2)$-representation ρ of $\mathcal{G}_C$. We consider an $SL(2)$-bundle $\tilde{E}$ over $\tilde{C}$, with flat connection, defined as follows: over the component $\tilde{C}_z$, $\tilde{E}$ is the trivial bundle $E_z \times \tilde{C}_z$, with its trivial connection. The desired $SL(2)$-bundle E over C with flat connection is then obtained by dividing out an equivalence relation: if $p = p'\wp$, we use $\rho(\wp)$ to identify the fibers of $\tilde{E}$ over p and p'.

Equivariant $GL(1)$-representations

By an equivariant $GL(1)$-representation ρ^{ab} of $\mathcal{G}_{\Sigma'}$ we mean

- a 1-dimensional vector space $\mathcal{L}_z$ for each $z \in \mathcal{P}_{\Sigma'}$,
- an isomorphism $\rho^{\mathrm{ab}}(\wp) : \mathcal{L}_{i(\wp)} \to \mathcal{L}_{f(\wp)}$ for each morphism $\wp$ of $\mathcal{G}_{\Sigma'}$, with initial point $i(\wp)$ and final point $f(\wp)$; ρ^{ab} should be compatible with composition,
- a nondegenerate pairing $\mu_z : \mathcal{L}_z \otimes \mathcal{L}_{\sigma(z)} \to \mathbb{C}$ for each $z \in \mathcal{P}_\Sigma$, with the antisymmetry property $\mu(s, s') = -\mu(\sigma^* s', \sigma^* s)$, and compatible with ρ^{ab} in the obvious sense.

In parallel to the previous section we can also define *equivalence* of equivariant $GL(1)$-representations: the only new point is that an equivalence between ρ^{ab} and ρ'^{ab} is required to intertwine μ and μ' in the obvious sense. Then, again in parallel to the previous section, there is an equivalence between the category of equivariant $GL(1)$-representations of $\mathcal{G}_{\Sigma'}$ and the category of equivariant $GL(1)$-connections over Σ'. (The construction is just as above, now using the path space $\tilde{\Sigma}'$ instead of $\tilde{C}$; the equivariant structure goes through straightforwardly.)

Just as for equivariant $GL(1)$-connections over Σ', equivariant $GL(1)$-representations are automatically almost-flat, in the sense that they assign holonomy -1 to a loop around a branch point.

Representation $\mathcal{W}$-pairs

Now we are ready to define the integrated analogue of a $\mathcal{W}$-pair. These definitions will be parallel to those of §4.1.

As before, suppose we have fixed a spectral network $\mathcal{W}$ subordinate to a covering Σ. Then:

- A *representation $\mathcal{W}$-pair* is a tuple $(\rho, \rho^{\mathrm{ab}}, \iota)$, consisting of:
  - an $SL(2)$-representation ρ of $\mathcal{G}_C$,

[15] Notice that our notation for composing paths is opposite from usual: if the end point of $\wp_1$ agrees with the initial point of $\wp_2$, we write their composition as $\wp_2\wp_1$.

- an equivariant $GL(1)$-representation ρ^{ab} of $\mathcal{G}_{\Sigma'}$,
- an isomorphism $\iota_z : E_z \to (\pi_* \mathcal{L})_z$ for each $z \in \mathcal{P}_C$,

such that

- if $\wp$ does not cross any walls of $\mathcal{W}$, then ι intertwines $\pi_* \rho^{\mathrm{ab}}(\wp)$ with $\rho(\wp)$:

$$\rho(\wp) = \iota^{-1}_{f(\wp)} \circ \pi_* \rho^{\mathrm{ab}}(\wp) \circ \iota_{i(\wp)}, \tag{6.3}$$

- if $\wp$ is a short path connecting the two basepoints attached to a wall w of $\mathcal{W}$, then ι intertwines $\pi_* \rho^{\mathrm{ab}}(\wp)$ with $\rho(\wp)$ up to a unipotent correction:

$$\rho(\wp) = \iota^{-1}_{f(\wp)} \circ \mathcal{S}_w \circ \pi_* \rho^{\mathrm{ab}}(\wp) \circ \iota_{i(\wp)} \tag{6.4}$$

  where $\mathcal{S}_w$ is a unipotent endomorphism of $(\pi_* \mathcal{L})_z$: if w carries the label ij then we have $\mathcal{S}_w = 1 + e_w$, where $e_w : \mathcal{L}_{z^{(i)}} \to \mathcal{L}_{z^{(j)}}$,
- the pairing μ_z corresponds to the volume form ε_z under the isomorphism ι_z.

- Given a flat $SL(2)$-representation ρ of the path groupoid $\mathcal{G}_C$ on C, a *$\mathcal{W}$-abelianization* of ρ is any extension of ρ to a representation $\mathcal{W}$-pair $(\rho, \rho^{\mathrm{ab}}, \iota)$.
- Given an equivariant $GL(1)$-representation ρ^{ab} of $\mathcal{G}_{\Sigma'}$ on Σ, a *$\mathcal{W}$-nonabelianization* of ρ^{ab} is any extension of ρ^{ab} to a representation $\mathcal{W}$-pair $(\rho, \rho^{\mathrm{ab}}, \iota)$.

An *equivalence* between representation $\mathcal{W}$-pairs $(\rho, \rho^{\mathrm{ab}}, \iota)$ and $(\rho', \rho'^{\mathrm{ab}}, \iota')$ is a pair (g, g^{ab}) where g is an equivalence between ρ and ρ' as defined above, and g^{ab} an equivalence between ρ^{ab} and ρ'^{ab} as defined above, such that g and g^{ab} intertwine ι with ι'.

We have now defined a category of representation $\mathcal{W}$-pairs. Naturally, the point of the definition is that this category is equivalent to the category of ordinary $\mathcal{W}$-pairs which we defined in §4.1 above. The construction of this equivalence is completely parallel to the constructions for the individual categories of representations which we considered above.

Representations with boundary and gluing

If C has boundary, it is sometimes useful to consider representations and representation $\mathcal{W}$-pairs with a bit of extra structure. The definitions in §4.3 translate to the following.

- An $SL(2)$-representation with boundary consists of an $SL(2)$-representation together with a trivialization of E_z for each marked point z.
- An equivariant $GL(1)$-representation with boundary consists of an equivariant $GL(1)$-representation together with a trivialization of $\mathcal{L}_z$ for each marked point z.
- A representation $\mathcal{W}$-pair with boundary is a tuple $(\rho, \rho^{\mathrm{ab}}, \iota)$ consisting of an $SL(2)$-representation with boundary ρ, an equivariant $GL(1)$-representation with boundary ρ^{ab}, and a trivialization of the covering Σ over each marked point z such that the isomorphism ι maps the trivialization of E_z to the trivialization of $\pi_* \mathcal{L}_{z_i}$ induced from those of $\mathcal{L}_{z_i}$ and Σ.

Given two surfaces C, C' with boundary, we can then define the gluing of two $SL(2)$-representations or two representation $\mathcal{W}$-pairs with boundary, parallel to the discussion in §4.3.

7 Constructing nonabelianizations

In this section, given a Fock-Goncharov or Fenchel-Nielsen spectral network $\mathcal{W}$ subordinate to a cover Σ, and an equivariant $GL(1)$-representation ρ^{ab} of $\mathcal{G}_{\Sigma'}$, we construct a $\mathcal{W}$-nonabelianization of ρ^{ab}.

First, for $z \in \mathcal{P}_C$ we define

$$E_z = (\pi_* \mathcal{L})_z, \tag{7.1}$$

and let ι_z be the identity map. (Up to equivalence, this choice does not involve any loss of generality: any $\mathcal{W}$-nonabelianization of ρ^{ab} is trivially equivalent to one for which $E_z = (\pi_* \mathcal{L})_z$ and ι_z is the identity.) The pairing μ_z induces a volume element $\varepsilon_z \in \wedge^2(E)$.

To complete the $\mathcal{W}$-nonabelianization, it only remains to determine the parallel transports $\rho(\wp)$. These are constrained by the intertwining relations (6.3), (6.4), which *almost* determine them in terms of the given ρ^{ab}: the only remaining ambiguity is in the choice of the e_w attached to the walls. Each e_w lies in a 1-dimensional vector space $Hom(\mathcal{L}_i, \mathcal{L}_j)$.

If we choose the e_w arbitrarily, the resulting elements $\rho(\wp)$ will not necessarily define an honest representation of $\mathcal{G}_C$: they will not satisfy the condition of homotopy invariance. Concretely, this condition amounts to requiring that $\rho(\wp) = 1$ whenever $\wp$ is a contractible loop on C. A general contractible loop $\wp$ on C can be written as a composition of loops which do not cross any walls and loops which encircle a single branch point. If $\wp$ does not cross any walls, then $\rho(\wp) = 1$ follows simply from (6.3) and the fact that ρ^{ab} is an honest representation of $\mathcal{G}_{\Sigma'}$. So it only remains to consider loops $\wp$ which encircle a single branch point: for each such loop, the condition $\rho(\wp) = 1$ gives a nontrivial constraint on the e_w, which we call a *branch point constraint*.

We will now show that, for all Fock-Goncharov or Fenchel-Nielsen networks $\mathcal{W}$, the branch point constraints admit a unique solution, and thus completely determine the e_w. For a Fock-Goncharov network, we consider the path $\wp$ in Figure 21. Since $\wp$ is

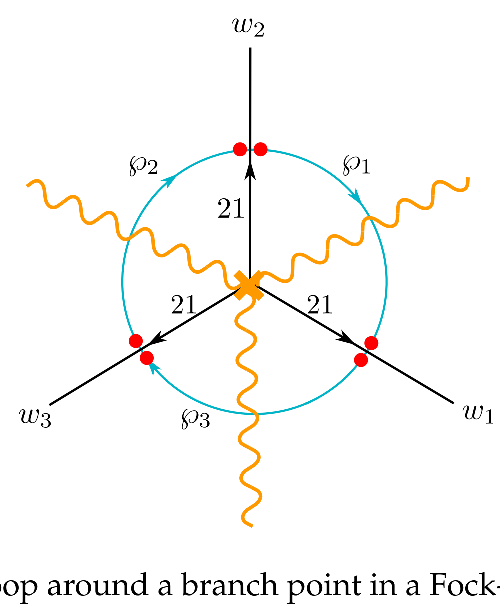

Figure 21: A small loop around a branch point in a Fock-Goncharov network.

contractible, we must have

$$\rho(\wp) = 1. \tag{7.2}$$

On the other hand, using (6.3), (6.4) we have

$$\rho(\wp) = \mathcal{S}_{w_1} \circ \pi_* \rho^{\mathrm{ab}}(\wp_1) \circ \mathcal{S}_{w_2} \circ \pi_* \rho^{\mathrm{ab}}(\wp_2) \circ \mathcal{S}_{w_3} \circ \pi_* \rho^{\mathrm{ab}}(\wp_3) \tag{7.3}$$
$$= \begin{pmatrix} 1 & e_{w_1} \\ 0 & 1 \end{pmatrix} \begin{pmatrix} 0 & D_1 \\ D_1' & 0 \end{pmatrix} \begin{pmatrix} 1 & e_{w_2} \\ 0 & 1 \end{pmatrix} \begin{pmatrix} 0 & D_2 \\ D_2' & 0 \end{pmatrix} \begin{pmatrix} 1 & e_{w_3} \\ 0 & 1 \end{pmatrix} \begin{pmatrix} 0 & D_3 \\ D_3' & 0 \end{pmatrix} \tag{7.4}$$

where each matrix is written with respect to the decomposition of $\pi_* \mathcal{L}$ into the two lines $\mathcal{L}_i$, and D_n, D_n' are obtained by applying ρ^{ab} to the two lifts of $\wp_n$. Combining (7.2) and (7.4), and using the fact that $D_1 D_2' D_3 D_1' D_2 D_3' = -1$, gives the unique solution

$$e_{w_1} = -D_1 D_2' D_3, \qquad e_{w_2} = -D_2 D_3' D_1, \qquad e_{w_3} = -D_2 D_1' D_3. \tag{7.5}$$

Incidentally, this solution has a nice interpretation: it says that $-e_w$ is obtained by applying ρ^{ab} to a "detour" path on Σ, shown in Figure 22 for the wall $w = w_1$. This was the point of view taken in [1].

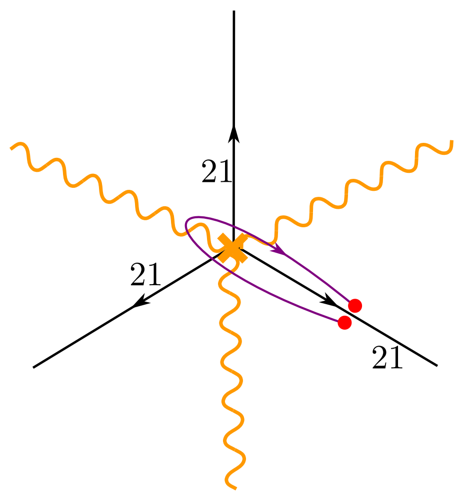

Figure 22: A "detour" path on Σ.

Next suppose we have a Fenchel-Nielsen network. In this case the walls are grouped into molecules of the shapes shown above in Figure 6. Let us consider molecule II as shown in Figure 23. Here we have 6 undetermined $e_{w_1}, \ldots, e_{w_6}$, 2 constraint equations (see footnote 15 for our convention on composing paths)

$$\rho(\wp_1 \wp_2 \wp_3) = 1, \qquad \rho(\wp_4 \wp_5 \wp_6) = 1, \tag{7.6}$$

and relations $D_1 D_1' D_2 D_2' D_3 D_3' = -1$ and $D_4 D_4' D_5 D_5' D_6 D_6' = -1$, just in parallel to the above. The equations (7.6) determine the e_{w_i} uniquely; for example one gets

$$e_{w_3} = D_1 D_3' \frac{1}{D_2 - D_2'} \tag{7.7}$$

where in writing the last factor we use the fact that D_2 and D_2' are just *numbers*, obtained by applying ρ^{ab} to *closed* paths. The other e_{w_i} are given by similar (slightly more complicated) expressions.

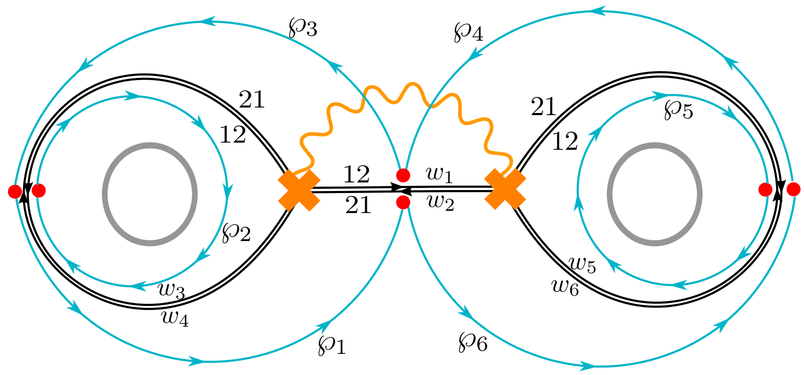

Figure 23: Local configuration around branch-points in a Fenchel-Nielsen molecule.

Thus, for any Fock-Goncharov or Fenchel-Nielsen network $\mathcal{W}$, there exists a (unique up to equivalence) $\mathcal{W}$-nonabelianization for any ρ^{ab}. Moreover, all our constructions were canonical; from this it easily follows that given an equivalence between equivariant $GL(1)$-connections ρ^{ab} and ρ'^{ab} we get an equivalence of their $\mathcal{W}$-nonabelianizations.

Fenchel-Nielsen with boundary

As a small extension of the above, suppose that $\mathcal{W}$ is a Fenchel-Nielsen network subordinate to a cover Σ with boundary. Suppose moreover that we are given an equivariant $GL(1)$-representation with boundary. Then we can easily extend the nonabelianization construction to construct a $\mathcal{W}$-pair with boundary.

Suppose that we are given two covers Σ, Σ' with boundary and an equivariant $GL(1)$-representation on each of Σ and Σ' with trivialization at the two preimages of a marked point z. If the monodromies around the glued components are the same (when written relative to the trivializations), then we can either first $\mathcal{W}$-nonabelianize and then glue the resulting $\mathcal{W}$-pairs, or first glue the two abelian $GL(1)$-representations and then $\mathcal{W}$-nonabelianize.

8 Moduli spaces and spectral coordinates

8.1 Moduli spaces

Given the surface C and a spectral network $\mathcal{W}$ of Fock-Goncharov or Fenchel-Nielsen type, subordinate to a covering Σ, we have considered three closely related categories. Now we consider the corresponding moduli spaces:

- let $\mathcal{M}(C, SL(2), \mathcal{W})$ be the moduli space parametrizing flat $\mathcal{W}$-framed $SL(2)$-connections over C, up to equivalence,
- let $\mathcal{M}(\Sigma, GL(1))$ be the moduli space parametrizing equivariant $GL(1)$-connections over Σ up to equivalence,
- let $\mathcal{M}(\mathcal{W})$ be the moduli space parameterizing $\mathcal{W}$-pairs up to equivalence.

The constructions of the last few sections lead to a diagram relating these spaces, as follows:

$$\begin{tikzcd}
& \mathcal{M}(\mathcal{W}) \arrow[dl, shift left, "\pi_1"] \arrow[dr, shift left, "\pi_2"] & \\
\mathcal{M}(\Sigma, GL(1)) \arrow[ur, shift left, "\psi_1"] & & \mathcal{M}(C, SL(2), \mathcal{W}) \arrow[ul, shift left, "\psi_2"]
\end{tikzcd}$$

Here,

- π_1 and π_2 are the *forgetful* maps which map a $\mathcal{W}$-pair to the underlying equivariant $GL(1)$-connection or $\mathcal{W}$-framed flat $SL(2)$-connection respectively,
- ψ_1 is the *nonabelianization* map constructed in §7, which extends an equivariant $GL(1)$-connection to a $\mathcal{W}$-pair,
- ψ_2 is the *abelianization* map constructed in §5, which extends a $\mathcal{W}$-framed flat $SL(2)$-connection to a $\mathcal{W}$-pair.

From this description it is evident that $\pi_1 \circ \psi_1$ and $\pi_2 \circ \psi_2$ are the identity maps. Moreover, the uniqueness we have proven for abelianization and nonabelianization say that π_1 and π_2 are both injective. It follows that all of the maps are bijections. In particular, $\Psi = \pi_1 \circ \psi_2$ is a bijection (in fact diffeomorphism)

$$\Psi : \mathcal{M}(C, SL(2), \mathcal{W}) \to \mathcal{M}(\Sigma, GL(1)). \tag{8.1}$$

Let us verify that the dimensions match. The dimension of the moduli space $\mathcal{M}(\Sigma, GL(1))$ is $2g' - 2g + n$, where g' and g are the genera of $\bar{\Sigma}$ and $\bar{C}$ respectively, and n the number of punctures or boundary components. Using the fact that the number of branch points is $-2\chi(C)$ (proven in §2.1), we get $\chi(\bar{\Sigma}) = 4\chi(\bar{C})$, which implies $2g' = -6 + 8g + 2n$. Thus we get

$$\dim \mathcal{M}(\Sigma, GL(1)) = 6g - 6 + 3n \tag{8.2}$$

indeed matching $\dim \mathcal{M}(C, SL(2), \mathcal{W}) = -3\chi(C)$, as desired. If we fix the conjugacy classes of the monodromies around the punctures on C then we get a similar matching with both dimensions reduced by n.

8.2 Spectral coordinates

Given an equivariant $GL(1)$-connection ∇^{ab} we can construct some interesting numbers, as follows. Given any class $\gamma \in H_1(\Sigma', \mathbb{Z})$ we can consider the holonomy

$$\mathcal{X}_\gamma = \mathrm{Hol}_\gamma \nabla^{\mathrm{ab}} \in \mathbb{C}^\times. \tag{8.3}$$

From their definition it immediately follows that they are multiplicative:

$$\mathcal{X}_\gamma \mathcal{X}_{\gamma'} = \mathcal{X}_{\gamma+\gamma'}. \tag{8.4}$$

Moreover, if γ_b denotes a small loop around a branch point b, then we have

$$\mathcal{X}_{\gamma_b} = -1. \tag{8.5}$$

Finally, the equivariance of ∇^{ab} implies the relation

$$\mathcal{X}_{\gamma+\sigma_*\gamma} = 1. \tag{8.6}$$

It follows from (8.4), (8.5), (8.6) that if we fix a collection $\{\gamma_i\} \subset H_1(\Sigma', \mathbb{Z})$ which generates $H_1(\Sigma', \mathbb{Z})/\langle \gamma + \sigma_*\gamma \rangle$, then the $\mathcal{X}_{\gamma_i}$ are enough to determine all of the $\mathcal{X}_\gamma$. They thus give a coordinate system on $\mathcal{M}(\Sigma, GL(1))$.

Alternatively, via the diffeomorphism Ψ in (8.1), the $\mathcal{X}_\gamma$ can be thought of as functions on $\mathcal{M}(C, SL(2), \mathcal{W})$, and the $\mathcal{X}_{\gamma_i}$ as above give a coordinate system. With this in mind, we call the $\mathcal{X}_{\gamma_i}$ *spectral coordinates*.

Spectral coordinate systems have some nice properties which distinguish them from arbitrary coordinate systems. In particular, it was argued in [1] that they are *Darboux* coordinates, in the following sense. The moduli space $\mathcal{M}(SL(2), C, \mathcal{W})$ has a natural holomorphic Poisson structure, described e.g. in [22] (generalizing the symplectic structure which one gets when C is closed [23]). The functions $\mathcal{X}_\gamma$ have simple Poisson brackets with respect to this structure:

$$\{\mathcal{X}_\gamma, \mathcal{X}_{\gamma'}\} = \langle \gamma, \gamma' \rangle \mathcal{X}_{\gamma+\gamma'}, \tag{8.7}$$

where $\langle \cdot, \cdot \rangle$ denotes the intersection pairing on $H_1(\Sigma', \mathbb{Z})$. In particular, if we fix our basis $\{\gamma_i\}$ so that $\langle \cdot, \cdot \rangle$ is of the block form

$$\begin{pmatrix} 0 & 1_{r\times r} & 0 \\ -1_{r\times r} & 0 & 0 \\ 0 & 0 & 0_{m\times m} \end{pmatrix},$$

the spectral coordinates $\mathcal{X}_{\gamma_i}$ for $i = 1, \ldots, r$ are Darboux coordinates for the symplectic leaves of $\mathcal{M}(SL(2), C, \mathcal{W})$.

So far we have been rather general. In the next two sections we want to show how these general considerations recover concretely known Darboux coordinate systems on $\mathcal{M}(C, SL(2), \mathcal{W})$, namely the Fock-Goncharov and complexified Fenchel-Nielsen coordinates.

8.3 Fock-Goncharov coordinates from Fock-Goncharov networks

Suppose $\mathcal{W}$ is a Fock-Goncharov network. Then, given a $\mathcal{W}$-framed $SL(2)$-connection ∇, we have explained in §5.2 the construction of the corresponding equivariant $GL(1)$-connection ∇^{ab}. Now we will use this construction to compute some of the spectral coordinates.

Consider the cycle γ on Σ' shown in Figure 24. We would like to compute the holonomy $\mathcal{X}_\gamma$ of ∇^{ab} around γ. To compute $\mathcal{X}_\gamma$ it is convenient to split γ into two open paths and compute their parallel transports separately. Thus, consider a single branch point and an open path a on Σ, as shown in Figure 25. We aim to describe the parallel transport $\mathcal{X}_a$ of ∇^{ab} along a.

Let s_n denote some ∇-flat section of ℓ_n over the quadrilateral Q (recall that ℓ_n denotes the framing at the puncture z_n.) Similarly define s_k, s_l, s_m associated to the framings at the

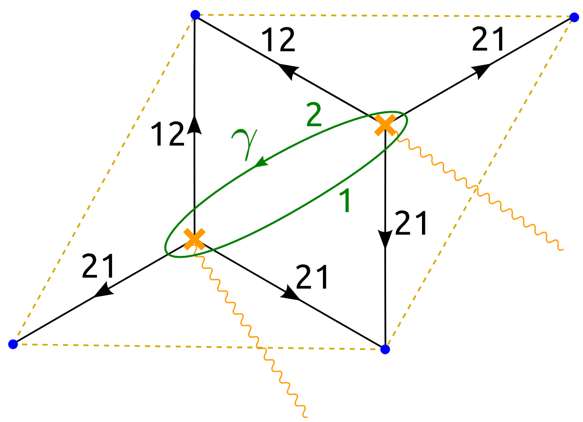

Figure 24: A canonical 1-cycle γ on Σ', lying above the pictured quadrilateral Q in C.

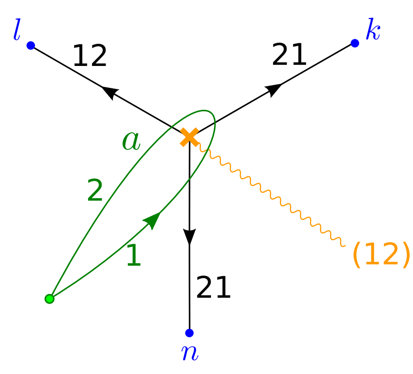

Figure 25: Path a around a branch point. The green labels 1 and 2 along the path refer to the sheets at which the path a starts and ends respectively.

other punctures. Since a is a path beginning on sheet 1 of Σ and ending on sheet 2, we have

$$\mathcal{X}_a(s_n) = \lambda s_l \tag{8.8}$$

for some scalar λ. Our job is to determine λ. For this, divide a into three segments $a = a_3 a_2 a_1$, each crossing one of the walls. Using $\mathcal{X}_a = \mathcal{X}_{a_3}\mathcal{X}_{a_2}\mathcal{X}_{a_1}$, (8.8) becomes

$$\mathcal{X}_{a_2}\mathcal{X}_{a_1}(s_n) = \lambda \mathcal{X}_{a_3^{-1}} s_l. \tag{8.9}$$

The triangular structure of the $\mathcal{S}_w$ says that we have $\mathcal{X}_{a_1}(s_n) = s_n$, $\mathcal{X}_{a_3}(s_l) = s_l$, so that we can simplify (8.9) to

$$\mathcal{X}_{a_2}(s_n) = \lambda s_l. \tag{8.10}$$

The triangular structure of the $\mathcal{S}_w$ also says $(\mathcal{X}_{a_2}(s_n) - s_n) \sim s_k$, which means $(\mathcal{X}_{a_2}(s_n) - s_n) \wedge s_k = 0$, i.e.

$$\lambda = \frac{s_n \wedge s_k}{s_l \wedge s_k}. \tag{8.11}$$

Now consider two neighboring branch points, as in Figure 26. The previous analysis

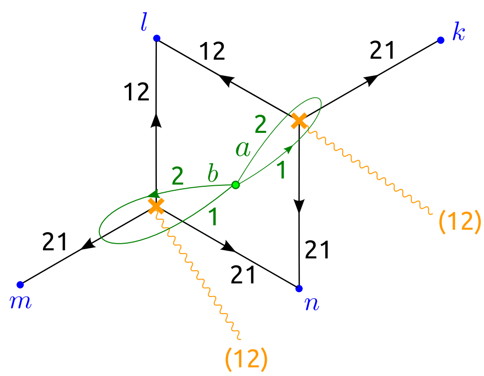

Figure 26: Cycle $\gamma = a + b$ in the quadrilateral Q with vertices k, l, m and n. The green labels 1 and 2 refer to sheets of the covering.

shows that

$$\mathcal{X}_a(s_n) = \frac{s_n \wedge s_k}{s_l \wedge s_k} s_l, \qquad \mathcal{X}_b(s_l) = \frac{s_l \wedge s_m}{s_n \wedge s_m} s_n. \tag{8.12}$$

Combining these gives

$$\mathcal{X}_a \mathcal{X}_b(s_l) = \frac{s_n \wedge s_k}{s_l \wedge s_k}\frac{s_l \wedge s_m}{s_n \wedge s_m} s_l, \tag{8.13}$$

but $a + b = \gamma$, so finally we can write the holonomy along the closed cycle γ:

$$\mathcal{X}_\gamma = \frac{(s_n \wedge s_k)(s_l \wedge s_m)}{(s_l \wedge s_k)(s_n \wedge s_m)}. \tag{8.14}$$

We emphasize that the expression (8.14) is $SL(2)$ invariant, and can be evaluated at any internal point of the quadrilateral Q. This is the main result of this section: it gives a concrete formula for the spectral coordinate $\mathcal{X}_\gamma$ attached to the cycle γ of Figure 24, in terms of data attached to the original $\mathcal{W}$-framed $SL(2)$-connection ∇.

This formula is a familiar one. Indeed, consider the ideal triangulation $\mathcal{T}$ which corresponds to the Fock-Goncharov network $\mathcal{W}$. The quadrilateral Q contains a unique edge of $\mathcal{T}$. On the other hand, for each edge of $\mathcal{T}$ there is a corresponding Fock-Goncharov coordinate on the space of $\mathcal{W}$-framed connections [9]. $\mathcal{X}_\gamma$ given by (8.14) is this Fock-Goncharov coordinate multiplied by -1. The sign discrepancy can be eliminated by shifting γ by a loop around a branch point, i.e. replacing γ by γ' shown in Figure 27.

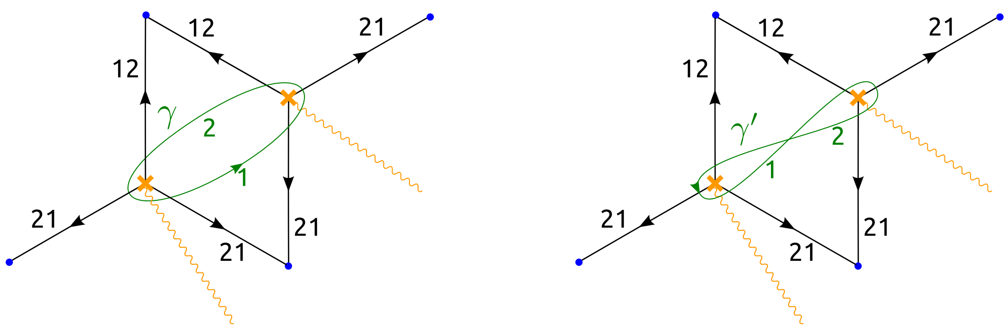

Figure 27: The homology classes γ and γ' differ only by the addition of a loop around one of the branch points on Σ. Thus $\mathcal{X}_{\gamma'} = -\mathcal{X}_\gamma$.

Applying this result to each cell in turn, we obtain a collection of cycles $\gamma_i \in H_1(\Sigma, \mathbb{Z})$ such that the spectral coordinates $\mathcal{X}_{\gamma_i}$ are the Fock-Goncharov coordinates attached to the ideal triangulation $\mathcal{T}$. We have thus rederived the result of [4] in the special case $K = 2$ (see also [3] where essentially the same result appeared, albeit phrased in a different language.)

Knowing the $\mathcal{X}_{\gamma_i}$ does not quite determine the $GL(1)$-connection ∇^{ab}. Indeed, the cycles γ_i descend to a $\mathbb{Q}$-basis for $H_1(\Sigma, \mathbb{Q})/\langle \gamma + \sigma_* \gamma \rangle$, but not necessarily to a $\mathbb{Z}$-basis for $H_1(\Sigma, \mathbb{Z})/\langle \gamma + \sigma_* \gamma \rangle$. Thus the full collection of all spectral coordinates $\mathcal{X}_\gamma$ contains slightly more information than the Fock-Goncharov coordinates $\mathcal{X}_{\gamma_i}$. This extra information is enough to determine the $SL(2)$-connection ∇ up to equivalence (whereas the Fock-Goncharov coordinates would be enough to determine only its projection to $PSL(2)$.) We will see how this works explicitly in some examples in §9.

8.4 Fenchel-Nielsen coordinates from Fenchel-Nielsen networks

Next, suppose $\mathcal{W}$ is a Fenchel-Nielsen network. Then, given a $\mathcal{W}$-framed $SL(2)$-connection ∇, we have explained in §5.3 the construction of the corresponding equivariant $GL(1)$-connection ∇^{ab}. Now we will use this construction to compute some of the spectral coordinates. We will see that they are essentially complexified Fenchel-Nielsen coordinates.

One new subtlety here is that, unlike the Fock-Goncharov case just considered, a Fenchel-Nielsen network does not quite give a basis for $H_1(\Sigma, \mathbb{Q})/\langle \gamma + \sigma_* \gamma \rangle$. Instead it gives a basis up to some shifts: more precisely, half of the basis elements are canonical (these will be associated to the Fenchel-Nielsen length coordinates, which are likewise canonical) while the other half are ambiguous by certain shifts (these will be associated to the Fenchel-Nielsen twist coordinates, which are likewise known to suffer from some ambiguities.)

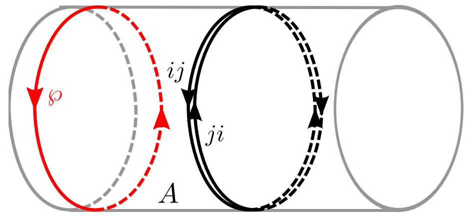

Figure 28: Cycle $\wp$ used to compute the spectral length coordinate associated to an annulus A. (Only the region near one boundary component of A is shown.)

Consider the annulus A pictured in Figure 28, and the path $\wp$ going around in the same direction as the nearest walls on the boundary (call this the $+$ direction). We choose a labeling of the sheets of Σ over A, such that the nearest boundary walls are of type ij. Let $\gamma \in H_1(\Sigma, \mathbb{Z})$ be the lift of $\wp$ to sheet j. The holonomy $\mathcal{X}_\gamma$ of ∇^{ab} along γ is equal to the eigenvalue of M_+ acting on the section s_j. According to our rules above, $s_j = s_+$. Thus $\mathcal{X}_\gamma$ is the monodromy eigenvalue corresponding to the section s_+. This monodromy eigenvalue is a complexified version of a square-root of the exponentiated Fenchel-Nielsen length coordinate of the connection ∇. Thus we have found that *square roots of complexified exponentiated Fenchel-Nielsen length coordinates arise as $GL(1)$ holonomies of ∇^{ab}.*

The cycles γ obtained in this way do not descend to a basis of $H_1(\Sigma, \mathbb{Q})/\langle \gamma + \sigma_* \gamma \rangle$. This corresponds to the fact that the exponentiated complexified Fenchel-Nielsen length coordinates do not give a complete coordinate system on the moduli of flat $PSL(2)$-connections. To get more cycles we now consider ones which cross the annuli, such as γ pictured in Figure 29.

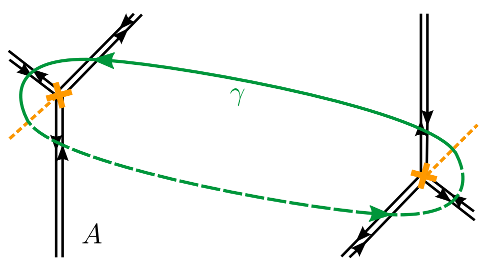

Figure 29: A local region of an annulus A, and a cycle $\gamma \in H_1(\Sigma, \mathbb{Z})$ which can be used to define the spectral twist coordinate associated to A.

How should we understand the $GL(1)$ holonomy $\mathcal{X}_\gamma$? Rather than trying to compute it directly, let us take a more indirect route: we want to consider how $\mathcal{X}_\gamma$ is transformed under a modification of the connection ∇, as follows. Suppose we cut the surface C into two pieces along the annulus A. We will obtain two surfaces with boundary, say C_1 and C_2, carrying connections ∇_1 and ∇_2, as well as an isomorphism $i : E_1 \simeq E_2$ along the boundary, with $\nabla_1 = i^* \nabla_2$. We could now glue C back together along the boundary using the isomorphism i to recover the original ∇. However, we could instead glue with an isomorphism $i' = i \circ a$, where a is any automorphism of E_1 which preserves ∇_1. Such an automorphism must preserve the monodromy eigenspaces: thus, in terms of the sections s_1, s_2 of E over A, the action of a can be written as $s_1 \to \lambda s_1$, $s_2 \to \lambda^{-1} s_2$. Thus we obtain a 1-parameter family of modified connections $\nabla(\lambda)$. This operation is sometimes called the "twist flow."

If the original connection ∇ is abelianized by ∇^{ab}, then $\nabla(\lambda)$ is also abelianized by a connection $\nabla^{\mathrm{ab}}(\lambda)$, constructed by the $GL(1)$ analogue of the twist flow: we cut Σ apart along the two components of $\pi^{-1}(A)$, then reglue using the automorphism $s \to \lambda s$ on sheet 1 and $s \to \lambda^{-1} s$ on sheet 2. From this description, it follows that the twist flow acts simply on the coordinate $\mathcal{X}_\gamma$:

$$\mathcal{X}_\gamma \mapsto \lambda^2 \mathcal{X}_\gamma. \tag{8.15}$$

One sees this by computing the parallel transport of $\nabla^{\mathrm{ab}}(\lambda)$ along γ: it is identical to that of ∇^{ab}, except for two extra factors of λ for the two times the path γ crosses $\pi^{-1}(A)$.

The transformation law (8.15) under twist flow is the characteristic property of a (complexified, exponentiated) "Fenchel-Nielsen twist coordinate."[16] We call it *a* twist coordinate rather than *the* twist coordinate because of the ambiguity mentioned above. To fix this ambiguity one needs some further choice beyond that of a pants decomposition. What we have seen here is that given a particular Fenchel-Nielsen network $\mathcal{W}$ and a particular choice of a cycle γ on Σ crossing the annulus (as in Figure 29), we get a particular way of fixing the ambiguity, and *the spectral coordinate* $\mathcal{X}_\gamma$ *is a complexified exponentiated Fenchel-Nielsen twist coordinate.* Changing the choice of γ while keeping the network $\mathcal{W}$ fixed multiplies the twist coordinate $\mathcal{X}_\gamma$ by a power of the exponentiated length coordinate.

The $GL(1)$ holonomies of ∇^{ab} contain slightly more information than the Fenchel-Nielsen coordinates. Indeed, the spectral coordinates determine the full $SL(2)$-connection ∇ up to equivalence, while the complexified Fenchel-Nielsen coordinates determine only its projection to $PSL(2)$. (One reflection of this is the fact that, as we have noted, the exponentiated complexified Fenchel-Nielsen length coordinate is equal to the *square* of the spectral coordinate $\mathcal{X}_\gamma$.) We will see how this works explicitly in the examples in §9.

8.5 Mixed coordinates

Finally we briefly discuss the mixed networks of §2.5 above. As we discussed in §5.5, we can construct $\mathcal{W}$-abelianizations in this case just as for Fock-Goncharov or Fenchel-Nielsen networks. We expect that the spectral coordinates in this situation will be a kind of hybrid between Fock-Goncharov and Fenchel-Nielsen coordinate systems on the relevant $\mathcal{W}$-framed moduli spaces; these hybrid coordinate systems should contain some coordinates of each kind, along with new types of coordinates. We have not worked this story out in detail.

[16] We thank Anna Wienhard for emphasizing this point of view on the Fenchel-Nielsen coordinates.

9 Monodromy representations

In this section we discuss a few instructive examples of the nonabelianization construction. In particular, we verify that the nonabelianization map is injective, and give an interpretation of the unipotent elements $\mathcal{S}_w$. Furthermore, these examples clarify how the construction depends on whether we consider connections for the group $SL(2)$ or $PSL(2)$.

We start this section by outlining how the computations work in practice. That is, we explain how the somewhat formal description in §7 can be turned into a very concrete matrix calculation. The first result of this exercise is an explicit description of the space of equivariant $GL(1)$-representations. The second result is an explicit description of the nonabelianization map, which turns equivariant $GL(1)$-representations into $\mathcal{W}$-pairs. As a byproduct we find the monodromy representation of the corresponding $SL(2)$-representations in terms of spectral coordinates.

9.1 Strategy

As before we fix a branched covering $\Sigma \to C$ and a spectral network $\mathcal{W}$. But now we also make a choice of branch cuts and trivialize Σ.

We furthermore choose a set of generators for the paths in $\mathcal{G}_C$ such that they either do not cross any walls, or are short paths connecting the two basepoints attached to a single wall. We label the former generators as $\wp_n$, and call them *simple*, and label the latter generators as w_k (by slight abuse of notation). Their lifts to Σ form a set of generators for the paths in $\mathcal{G}_{\Sigma'}$. We denote them as $\wp_n^{(ij)}$ and $w_k^{(ii)}$, respectively.[17]

Our first aim is to give an explicit characterization of the space of equivariant $GL(1)$-representations.

An equivariant representation ρ^{ab} can be "trivialized" by choosing a basis vector $e_{z^{(i)}}$ in each line $\mathcal{L}_{z^{(i)}}$. We require these choices to be compatible with the equivariant structure, i.e. such that over each point $z \in \mathcal{P}_C$ the two elements $e_{z^{(1)}}$, $e_{z^{(2)}}$ obey the condition $\mu(e_{z^{(1)}}, e_{z^{(2)}}) = 1$. In this trivialization ρ^{ab} is simply given by a collection of $SL(2)$-valued matrices $\mathcal{D}_{\wp_n}$. One for each generating path $\wp_n$, where $\mathcal{D}_{\wp_n}$ is (off-)diagonal if $\wp_n$ crosses an even (odd) number of branch cuts.

Explicitly, for a simple generating path $\wp_n^{(ij)}$ the isomorphism $\rho^{\mathrm{ab}}(\wp_n^{(ij)})$ is just given by multiplication with the element

$$(\mathcal{D}_{\wp_n})_{ij},$$

whereas for a short generating path $w_k^{(ii)}$ it is simply the identity. When $\wp$ is not simple, for example $\wp = \wp_3 w_2 \wp_1$, and has a lift $\wp^{(ij)} = \wp_3^{(ik)} w_2^{(kk)} \wp_1^{(kj)}$, the isomorphism

$$\rho^{\mathrm{ab}}(\wp^{(ij)}) = \rho^{\mathrm{ab}}(\wp_3^{(ik)})\rho^{\mathrm{ab}}(w_2^{(kk)})\rho^{\mathrm{ab}}(\wp_1^{(kj)})$$

corresponds to multiplication with

$$(\mathcal{D}_{\wp_3})_{ik}(\mathcal{D}_{\wp_1})_{kj} = (\mathcal{D}_{\wp_3}\mathcal{D}_{\wp_1})_{ij}.$$

[17] Our conventions are such that $\wp_n^{(ij)}$ is a path that starts at sheet j and ends at sheet i.

There is an obvious extension to longer paths.

Two different trivializations $\mathcal{D}_{\wp_n}$ and $\mathcal{D}'_{\wp_n}$ of ρ^{ab} are related by an *abelian gauge transformation* $g : \mathcal{P}_C \to \mathbb{C}^\times$. If we label the initial point of the generating path $\wp_n$ by a number $i(n)$ and its final point by a number $f(n)$, this gauge transformation acts as

$$d_n \to d_n \frac{g_{i(n)}}{g_{f(n)}} \tag{9.1}$$

on a diagonal matrix $\mathcal{D}_{\wp_n}$, with entries d_n and d_n^{-1}, and as

$$d_n \to d_n \, g_{i(n)} \, g_{f(n)} \tag{9.2}$$

on a strictly off-diagonal matrix $\mathcal{D}_{\wp_n}$.

The other way around, a collection of matrices $\mathcal{D}_{\wp_n}$ can only be interpreted as the trivialization of an equivariant $GL(1)$-representation if there is no monodromy around contractible cycles on Σ'. We say in that case that the *bulk constraints* are satisfied. Indeed, we can construct an equivariant $GL(1)$-representation ρ^{ab} from such a collection by taking a copy of $\mathbb{C}$ for each line $\mathcal{L}_z$ and by defining the isomorphisms $\rho^{\mathrm{ab}}(\wp)$ through multiplication with $\mathcal{D}_{\wp_n}$.

First trivializing an equivariant $GL(1)$-representation ρ^{ab} into a collection of matrices $\mathcal{D}_{\wp_n}$ obeying the bulk constraints, and then constructing an equivariant $GL(1)$-representation from this collection, yields an equivariant $GL(1)$-representation ρ'^{ab} that is equivalent to ρ^{ab}. On the other hand, if we start with a collection of matrices $\mathcal{D}_{\wp_n}$ obeying the bulk constraints, turn this into a representation ρ^{ab} and then trivialize again, we find a new collection of matrices $\mathcal{D}'_{\wp_n}$ related by an abelian gauge transformation.

We have thus obtained an explicit characterization of the space of equivariant $GL(1)$-representations in terms of a collection of matrices $\mathcal{D}_{\wp_n}$ obeying the bulk constraints. Up to abelian gauge transformations the only parameters that enter the matrices $\mathcal{D}_{\wp_n}$ are spectral coordinates and holonomies around punctures on Σ.

Now we are ready to explicitly construct representation $\mathcal{W}$-pairs.

Given an equivariant $GL(1)$-representation ρ^{ab}, §7 prescribes how to obtain a $\mathcal{W}$-pair, and in particular an $SL(2)$-representation ρ (in “nonabelianization gauge”). Similar as before, we can trivialize this representation using the two basis vectors $e_{z^{(1)}}, e_{z^{(2)}}$ at every $z \in \mathcal{P}_C$. It follows that ρ can be explicitly described in terms of the matrices $\mathcal{D}_{\wp_n}$ as well, but with some additional unipotent matrices “spliced in”.

More precisely, introduce a normal vector for each wall w, a parameter $S_w \in \mathbb{C}$ and a matrix of the form

$$\mathcal{S}_w = \begin{cases} \begin{pmatrix} 1 & S_w \\ 0 & 1 \end{pmatrix} & \text{for } w \text{ of type 21,} \\ \begin{pmatrix} 1 & 0 \\ S_w & 1 \end{pmatrix} & \text{for } w \text{ of type 12.} \end{cases} \tag{9.3}$$

Then for any path $\wp \in \mathcal{G}_C$, the isomorphism $\rho(\wp)$ corresponds to multiplication by matrices $\mathcal{S}$ and $\mathcal{D}$. For example, when $\wp = w_1 \wp_2$ with w_1 a short path crossing the wall labeled by the same symbol and $\wp_2$ not crossing a wall, $\rho(\wp)$ is given by multiplication with

$$\mathcal{S}_{w_1} \mathcal{D}_{\wp_2}, \tag{9.4}$$

if the path $\wp$ runs in the direction of the normal vector attached to the wall w_1 that is being crossed. The extension to longer paths should be clear.

The fact that the matrices $\mathcal{D}_\wp$ obey the bulk constraints on Σ implies that they obey the bulk constraints on C as well. But if the numbers S_w are chosen arbitrarily, there is no reason to expect that the branch point constraints are obeyed. The arguments of §7 show that the branch point constraints can be solved uniquely for Fock-Goncharov and Fenchel-Nielsen networks. This determines the numbers S_w in terms of the matrices $\mathcal{D}_\wp$.

Thus, for each choice of abelian $GL(1)$-representation we obtain an explicit characterization of a unique representation $\mathcal{W}$-pair in terms of the matrices $\mathcal{D}_\wp$. In particular, we can compute the monodromy representation of the resulting $SL(2)$-representation in terms of purely abelian data.

Let us illustrate this with some examples.

9.2 Fock-Goncharov networks

First we describe nonabelianization for two examples of Fock-Goncharov networks, on the four-punctured sphere and on the one-punctured torus.

9.2.1 Four-punctured sphere

Consider the Fock-Goncharov network on the four-punctured sphere shown in Figure 5. We make a choice of basepoints $z_k \in \mathcal{P}_C$ and simple paths $\wp_m \in \mathcal{G}_C$ as in Figure 30. Along each simple path $\wp_m$ we choose an $SL(2)$ matrix $\mathcal{D}_{\wp_m}$ that is diagonal if the path has an even number of intersections with branch cuts and strictly off-diagonal if this number is odd. For instance,

$$\mathcal{D}_{\wp_1} = \begin{pmatrix} d_1 & 0 \\ 0 & d_1^{-1} \end{pmatrix}, \quad \mathcal{D}_{\wp_6} = \begin{pmatrix} 0 & -d_6^{-1} \\ d_6 & 0 \end{pmatrix}. \tag{9.5}$$

The collection of matrices $\mathcal{D}_{\wp_m}$ determines an equivariant abelian representation ρ^{ab}, provided that the bulk constraints are satisfied. We choose holonomies

$$M_{1,2}^{\mathrm{ab}} = \begin{pmatrix} \mathcal{X}_{1,2}^{-1} & 0 \\ 0 & \mathcal{X}_{1,2} \end{pmatrix} \tag{9.6}$$

in the clockwise direction around the lifts of the punctures $z_{1,2}$ to the cover Σ, and similarly holonomies

$$M_{3,4}^{\mathrm{ab}} = \begin{pmatrix} \mathcal{X}_{3,4} & 0 \\ 0 & \mathcal{X}_{3,4}^{-1} \end{pmatrix} \tag{9.7}$$

in the clockwise direction around the lifts of the punctures $z_{3,4}$ to the cover. Then we enforce the bulk equations, for instance

$$\mathcal{D}_{\wp_4}\mathcal{D}_{\wp_3}\mathcal{D}_{\wp_2}\mathcal{D}_{\wp_1} = M_1^{\mathrm{ab}}. \tag{9.8}$$

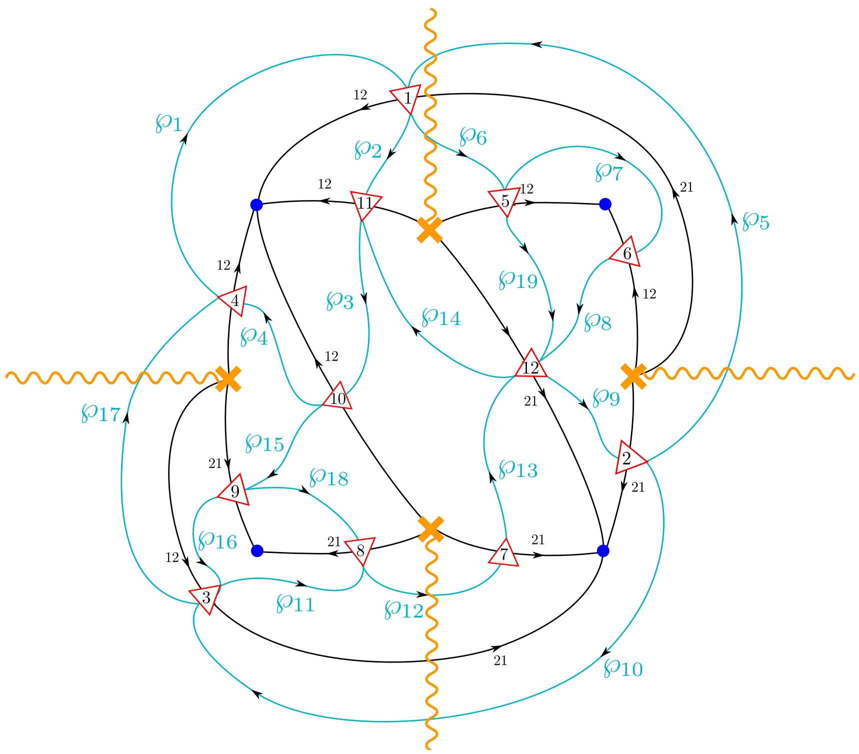

Figure 30: Spectral network on the four-punctured sphere with auxiliary data: blue lines are simple paths; the arrowhead and tail of the red arrows indicate the two base-points at either side of the wall; the direction of the red arrows specifies the normal vector at each wall.

There are four of these bulk equations, plus the equation at infinity

$$\mathcal{D}_{\wp_1 7}\mathcal{D}_{\wp_{10}}\mathcal{D}_{\wp_5}^{-1}\mathcal{D}_{\wp_1} = \mathbf{1}. \tag{9.9}$$

Thus the nineteen unknowns d_m are constrained by five equations in total, so that we have fourteen leftover degrees of freedom. This includes the gauge degrees of freedom, which we discussed around equation (9.1).

Fixing the abelian gauge freedom, i.e. choosing convenient values for the twelve g_k's, only leaves two degrees of freedom in the d_k's. These two unknowns correspond to gauge-invariant abelian holonomies around an A-cycle and B-cycle on the cover Σ. Let us call these abelian holonomies $\mathcal{X}_A$ and $\mathcal{X}_B$. In this example we may choose

$$\mathcal{X}_A = d_2\, d_{14}^{-1} d_9\, d_5 \quad \text{and} \quad \mathcal{X}_B = d_5^{-1} d_{10}\, d_{16}\, d_{15}\, d_3\, d_{14}\, d_8\, d_7\, d_6^{-1}. \tag{9.10}$$

Up to equivalence the equivariant $GL(1)$-representation ρ^{ab} is determined completely in terms of the abelian holonomies $\mathcal{X}_A, \mathcal{X}_B, \mathcal{X}_1, \ldots, \mathcal{X}_4$.

Having parametrized all equivariant $GL(1)$-representations on Σ, we now pick one of them and apply the non-abelianization construction.

We fix a normal vector at each basepoint z_k and write down a matrix $\mathcal{S}_k$ as in equation (9.3). The matrix $\mathcal{S}_k$ will determine the parallel transport across the wall in the direction of the normal vector.

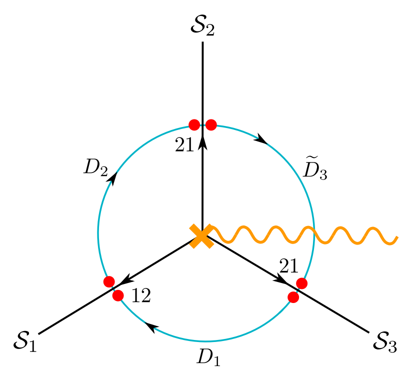

Figure 31: Local configuration around a branch point in a Fock-Goncharov network.

Requiring the $SL(2)$-representation ρ to be flat is equivalent to enforcing branch point constraints. There is one constraint for each branch point. For any branch point in a Fock-Goncharov network this constraint is of the form

$$\mathcal{S}_{3,ji}\widetilde{\mathcal{D}}_3\mathcal{S}_{2,ji}\mathcal{D}_2\mathcal{S}_{1,ij}\mathcal{D}_1 = \mathbf{1}, \tag{9.11}$$

where $\widetilde{\mathcal{D}}_3$ is a strictly off-diagonal matrix. See Figure 31. The $\mathcal{S}$-matrices that appear in this equation are fully determined by this constraint: their off-diagonal elements are of the form

$$S_{k,ij} = (\mathcal{D}_k\mathcal{D}_{k+2}\mathcal{D}_{k+1})_{ij}^{-1}, \tag{9.12}$$

where one of the matrices $\mathcal{D}$ has a tilde on it. (As noted before, this formula has a nice geometric interpretation: it represents the $GL(1)$ parallel transport along a path $a_k^{(ij)}$ that starts at the lift $z_k^{(j)}$, runs backward along the wall w^{ij} until it hits a branch point, loops around the branch point, then follows the wall w^{ij} forward to the lift $z_k^{(i)}$.)

Now that we have determined the $\mathcal{S}$-matrices, we have an explicit description of the $SL(2)$-representation ρ in terms of abelian data. In particular, we can compute the monodromies of ρ around any loop on C.

We fix a presentation of the fundamental group of C, i.e. four cycles $\mathcal{P}_1, \ldots, \mathcal{P}_4$ with a common basepoint, chosen such that $\mathcal{P}_p$ loops around the pth puncture, and with the relation $\mathcal{P}_4\mathcal{P}_3\mathcal{P}_2\mathcal{P}_1 = 1$. Then we compute the $SL(2)$ monodromies $\mathcal{M}_{\mathcal{W}}(\mathcal{P}_p)$ in terms of the abelian data. For instance, if we choose

$$\mathcal{P}_1 = w_{11}\wp_2 w_1 \wp_1 w_4 \wp_4 w_{10} \wp_3 \tag{9.13}$$

the corresponding monodromy matrix is obtained by splicing in the $\mathcal{S}$-matrices,

$$\begin{aligned} M_{\mathcal{W}}(\mathcal{P}_1) &= \mathcal{S}_{11}\mathcal{D}_{\wp_2}\mathcal{S}_1\mathcal{D}_{\wp_1}\mathcal{S}_4\mathcal{D}_{\wp_4}\mathcal{S}_{10}\mathcal{D}_{\wp_3} \\ &= \begin{pmatrix} \mathcal{X}_1^{-1} & 0 \\ g & \mathcal{X}_1 \end{pmatrix}, \end{aligned} \tag{9.14}$$

where g is a somewhat complicated expression that changes under abelian gauge transformations. We can easily check though that (in any gauge)

$$M_{\mathcal{W}}(\mathcal{P}_4) \cdot M_{\mathcal{W}}(\mathcal{P}_3) \cdot M_{\mathcal{W}}(\mathcal{P}_2) \cdot M_{\mathcal{W}}(\mathcal{P}_1) = 1, \tag{9.15}$$

and hence we have found the monodromy representation of the $SL(2)$-representation ρ on the four-punctured sphere, in terms of the abelian holonomies $\mathcal{X}_A$, $\mathcal{X}_B$, $\mathcal{X}_1, \ldots, \mathcal{X}_4$.

Complexified shear coordinates

So far we have constructed the $SL(2)$-representation ρ for a Fock-Goncharov network in terms of abelian data. Now let us discuss how the Fock-Goncharov coordinates are explicitly realized in terms of the abelian data.

Recall the definition of the Fock-Goncharov coordinates reviewed in §5.2, which assigns one Fock-Goncharov coordinate to each edge of the ideal triangulation corresponding to the network. In our case this triangulation has six edges; we label the Fock-Goncharov coordinates for these edges $\mathcal{Z}_1, \ldots, \mathcal{Z}_6$ as illustrated in Figure 32. For instance,

$$\mathcal{Z}_2 = \frac{(s_1 \wedge s_3')(s_2 \wedge s_3'')}{(s_2 \wedge s_3')(s_1 \wedge s_3'')}. \tag{9.16}$$

Here s_3' and s_3'' represent the parallel transport of the section s_3 along two inequivalent paths in the two triangles on either side of the edge labeled by the coordinate $\mathcal{Z}_2$.

Now, from the discussion of §5.2 we expect that the coordinates $\mathcal{Z}_1, \ldots, \mathcal{Z}_6$ can be expressed in terms of abelian holonomies along odd cycles on Σ. Concretely, for example,

$$\mathcal{Z}_2 = (\mathcal{D}_{\wp_9}\mathcal{D}_{\wp_8}\mathcal{D}_{\wp_7}\mathcal{D}_{\wp_{19}}^{-1}\mathcal{D}_{\wp_{14}}^{-1}\mathcal{D}_{\wp_2}\mathcal{D}_{\wp_5})_{22}.$$

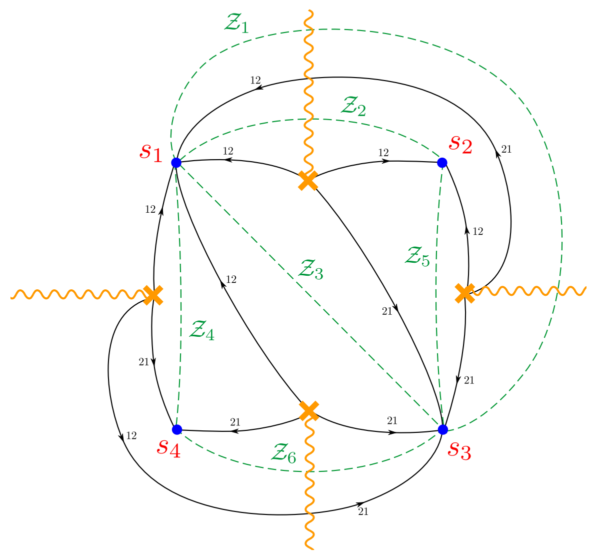

Figure 32: Ideal triangulation (in dark green) on the four-punctured sphere, and the corresponding shear coordinates $\mathcal{Z}_1, \ldots, \mathcal{Z}_6$.

In turn these holonomies can be expressed in terms of $\mathcal{X}_A, \mathcal{X}_B, \mathcal{X}_1, \ldots, \mathcal{X}_4$. Doing this we obtain

$$\mathcal{Z}_1 = \mathcal{X}_1\mathcal{X}_A\mathcal{X}_B, \quad \mathcal{Z}_2 = -\frac{\mathcal{X}_2}{\mathcal{X}_A}, \quad \mathcal{Z}_3 = \frac{\mathcal{X}_3}{\mathcal{X}_2\mathcal{X}_4\mathcal{X}_A\mathcal{X}_B},$$
$$\mathcal{Z}_4 = -\frac{\mathcal{X}_1\mathcal{X}_4\mathcal{X}_A}{\mathcal{X}_3}, \quad \mathcal{Z}_5 = -\mathcal{X}_2\mathcal{X}_A, \quad \mathcal{Z}_6 = -\frac{\mathcal{X}_3\mathcal{X}_4}{\mathcal{X}_1\mathcal{X}_A}. \tag{9.17}$$

As a check, the consecutive product of shear coordinates on the edges ending at the pth puncture is equal to $\mathcal{X}_p^2$.

If we attempt to invert the relations (9.17) to find the abelian holonomies ($\mathcal{X}$'s) in terms of the $\mathcal{Z}$'s, we find that the $\mathcal{X}$'s involve square roots in the $\mathcal{Z}$'s. This is consistent with the fact that the Fock-Goncharov coordinates $\mathcal{Z}$ do not completely determine an $SL(2)$-representation, only its projection to $PSL(2)$. In contrast, the $\mathcal{X}$'s really do determine the $SL(2)$-representation.

Rather than comparing only the gauge invariant quantities ($\mathcal{X}$'s and $\mathcal{Z}$'s) we can also go a bit further and compare the actual $SL(2)$ parallel transport matrices which we obtain by nonabelianization (depending on $\mathcal{X}$'s) to the ones given in the Fock prescription (depending on $\mathcal{Z}$'s). This prescription was given in [24] (see also Appendix A of [3]). Let us briefly review it.

We compute the monodromy matrix $M_{\mathcal{F}}(\mathcal{P}_p)$ as follows. Follow the loop $\mathcal{P}_p$ and write down a matrix

$$E(\mathcal{Z}_E) = \begin{pmatrix} 0 & 1 \\ \mathcal{Z}_E & 0 \end{pmatrix}, \tag{9.18}$$

when we cross an edge E labeled by the shear coordinate $\mathcal{Z}_E$. When turning right (left) inside a triangle, we write down the matrix V (V^{-1}) given by

$$V = \begin{pmatrix} -1 & 1 \\ -1 & 0 \end{pmatrix} \tag{9.19}$$

The monodromy matrix $M_{\mathcal{F}}(\mathcal{P}_p)$ is then the ordered product of the matrices $E(\mathcal{Z})$ and V, multiplied by a normalization factor which makes the determinant 1. For example, in our case

$$M_{\mathcal{F}}(\mathcal{P}_1) \quad = \pm \mathcal{X}_1^{-1} V E(\mathcal{Z}_2) V E(\mathcal{Z}_1) V E(\mathcal{Z}41) V E(\mathcal{Z}_3). \tag{9.20}$$

The normalization factor is only determined up to a sign, so the resulting $M_{\mathcal{F}}(\mathcal{P}_p)$ is really valued in $PSL(2)$. We want to compare the $M_{\mathcal{F}}(\mathcal{P}_p)$ with the matrices $M_{\mathcal{W}}(\mathcal{P}_p)$ which arise from nonabelianization, which are $SL(2)$-valued. Thus we fix the sign in $M_{\mathcal{F}}(\mathcal{P}_p)$ in such a way that the eigenvalues match. Denote the resulting $SL(2)$-valued matrices by $M^{\epsilon}_{\mathcal{F}}(\mathcal{P}_p)$. After so doing, we can indeed verify directly that the monodromy matrices $M^{\epsilon}_{\mathcal{F}}(\mathcal{P}_p)$ and $M_{\mathcal{W}}(\mathcal{P}_p)$ are conjugate.

This comparison also gives a concrete way of seeing how the reduction from $SL(2)$-representations to $PSL(2)$-representations works on the level of the spectral coordinates. Let us call the $SL(2)$-representation ρ, as before, and its reduction to a $PSL(2)$-representation $\tilde{\rho}$. The normalization factors of the Fock matrices $M_{\mathcal{F}}(\mathcal{P}_{1,2,3,4})$ are given by $1/\mathcal{X}_1$, $\mathcal{X}_2$, $\mathcal{X}_1/(\mathcal{X}_2\mathcal{X}_4)$ and $\mathcal{X}_4$, respectively, and are dependent on the choice of the lift of $\tilde{\rho}$ to ρ. In contrast, the shear coordinates $\mathcal{Z}_E$ should only depend on $\tilde{\rho}$. This suggests that any two lifts of $\tilde{\rho}$ to $SL(2)$ are related to one another by a transformation

$$\begin{aligned} \mathcal{X}_1 &\mapsto \epsilon_1\, \mathcal{X}_1\,, \\ \mathcal{X}_2 &\mapsto \epsilon_2\, \mathcal{X}_2\,, \\ \mathcal{X}_4 &\mapsto \epsilon_3\, \mathcal{X}_4\,, \end{aligned} \tag{9.21}$$

for a choice of $\epsilon_1, \epsilon_2, \epsilon_3 \in \{\pm 1\}$. Indeed, from the relations (9.17) it is easy to see that this operation can be uniquely completed to a transformation on all the $GL(1)$ holonomies $\mathcal{X}_A$, $\mathcal{X}_B$, $\mathcal{X}_1, \ldots, \mathcal{X}_4$, in such a way that the shear coordinates $\mathcal{Z}_E$ are invariant.

We call two equivariant $GL(1)$-representations $PSL(2)$-equivalent if they are related by a transformation of this kind. Then we find a 1-1 correspondence between equivariant $GL(1)$-representations, up to $PSL(2)$-equivalence, and $PSL(2)$-representations.

9.2.2 Once-punctured torus

Next, we work out the nonabelianization map for a Fock-Goncharov network on the once-punctured torus. Figure 33 illustrates the chosen spectral network with auxiliary data such as basepoints and simple paths.

We choose an $SL(2)$ matrix $\mathcal{D}_{\wp}$ for each simple path $\wp$. This matrix is diagonal if the path has an even number of intersections with branch cuts and strictly off-diagonal if this number is odd. Altogether these matrices contain 9 degrees of freedom $d_{\wp}$.

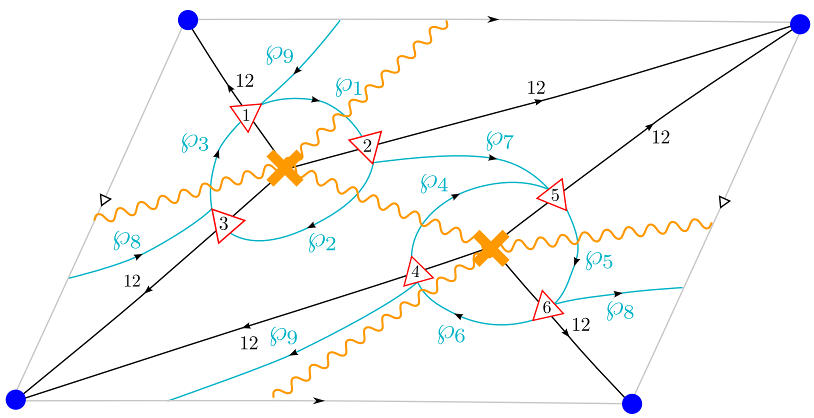

Figure 33: Spectral network on the once-punctured torus with auxiliary data.

The collection of matrices $\mathcal{D}_\wp$ determines an equivariant $GL(1)$-representation ρ^{ab} iff the matrices obey the bulk constraints. In this example there are three bulk equations:

$$\begin{aligned} M_a^{\mathrm{ab}} &= \mathcal{D}_4^{-1}\mathcal{D}_7\mathcal{D}_1\mathcal{D}_9, \\ M_b^{\mathrm{ab}} &= \mathcal{D}_5\mathcal{D}_7\mathcal{D}_2^{-1}\mathcal{D}_8, \\ M_m^{\mathrm{ab}} &= \mathcal{D}_5\mathcal{D}_7\mathcal{D}_1\mathcal{D}_9\mathcal{D}_6\mathcal{D}_8^{-1}\mathcal{D}_2\mathcal{D}_7^{-1}\mathcal{D}_4\mathcal{D}_9^{-1}\mathcal{D}_3\mathcal{D}_8, \end{aligned} \tag{9.22}$$

where we define

$$M_{a,b,m}^{\mathrm{ab}} = \begin{pmatrix} \mathcal{X}_{a,b,m} & 0 \\ 0 & \mathcal{X}_{a,b,m}^{-1} \end{pmatrix}. \tag{9.23}$$

Each equation fixes the abelian holonomy around the lifts of a 1-cycle on the once-punctured torus to the covering. This completely fixes the equivariant $GL(1)$-representations on the once-punctured torus in terms of the abelian holonomies $\mathcal{X}_a$, $\mathcal{X}_b$ and $\mathcal{X}_m$.

The next step is to apply the nonabelianization construction. This works similar to the previous example. For any abelian $GL(1)$-representation, we can determine the $\mathcal{S}$-matrices using the branch point equations and find the resulting $SL(2)$-representation ρ in terms of abelian data.

Given a presentation of the fundamental group of the once-punctured torus, we can then compute the corresponding $SL(2)$ monodromy matrices $M_\mathcal{W}(\mathcal{P}_{a,b,m})$. For instance, if we fix three cycles $\mathcal{P}_a$, $\mathcal{P}_b$ and $\mathcal{P}_m$ with the relation

$$\mathcal{P}_b^{-1}\mathcal{P}_a^{-1}\mathcal{P}_b\mathcal{P}_a = \mathcal{P}_m, \tag{9.24}$$

we indeed verify that

$$M_\mathcal{W}(\mathcal{P}_b)^{-1}M_\mathcal{W}(\mathcal{P}_a)^{-1}M_\mathcal{W}(\mathcal{P}_b)M_\mathcal{W}(\mathcal{P}_a) = M_\mathcal{W}(\mathcal{P}_m). \tag{9.25}$$

For example,

$$\begin{aligned} M_\mathcal{W}(\mathcal{P}_a) &= \mathcal{S}_2\mathcal{D}_1\mathcal{D}_9\mathcal{S}_4^{-1}\mathcal{D}_4^{-1}\mathcal{D}_7 \\ &= \begin{pmatrix} \mathcal{X}_a^{-1} & \mathcal{X}_a\mathcal{X}_b^2\mathcal{X}_m^{-1}g^{-1} \\ g\mathcal{X}_a^{-1} & \mathcal{X}_a(\mathcal{X}_b^2+\mathcal{X}_m)\mathcal{X}_m^{-1} \end{pmatrix}, \end{aligned} \tag{9.26}$$

where g is a gauge-dependent quantity.

As in the previous example, we might compare these monodromy matrices with those which arise from the Fock prescription. There are three shear coordinates $\mathcal{Z}_{1,2,3}$ on the once-punctured torus. Expressed in terms of the abelian holonomies $\mathcal{X}_{a,b,m}$ they read

$$\mathcal{Z}_1 = \mathcal{X}_a^2 \mathcal{X}_m^{-1}, \quad \mathcal{Z}_2 = \mathcal{X}_b^2 \mathcal{X}_m^{-1}, \quad \mathcal{Z}_3 = \mathcal{X}_m \mathcal{X}_a^{-2} \mathcal{X}_b^{-2}. \tag{9.27}$$

Notice that even though $\mathcal{X}_m$ can be expressed as a ratio of shear coordinates, $\mathcal{X}_a$ and $\mathcal{X}_b$ cannot.

We compute the Fock matrices $M^s_{\mathcal{F}}(\mathcal{P}_{a,b,m})$ as

$$\begin{aligned}
M^+_{\mathcal{F}}(\mathcal{P}_a) &= \mathcal{X}_a V^{-1} E(\mathcal{Z}_2) V E(\mathcal{Z}_3), \\
M^+_{\mathcal{F}}(\mathcal{P}_b) &= \mathcal{X}_b V E(\mathcal{Z}_1) V^{-1} E(\mathcal{Z}_2), \\
M^+_{\mathcal{F}}(\mathcal{P}_b) &= M^+_{\mathcal{F}}(\mathcal{P}_b)^{-1} M^+_{\mathcal{F}}(\mathcal{P}_a)^{-1} M^+_{\mathcal{F}}(\mathcal{P}_b) M^+_{\mathcal{F}}(\mathcal{P}_a),
\end{aligned}$$

and compare them to the spectral matrices $M_{\mathcal{W}}(\mathcal{P}_{a,b,m})$. As before, we find that the two sets of matrices are conjugate.

We can reduce from $SL(2)$ to $PSL(2)$-representations by considering transformations

$$\begin{aligned}
\mathcal{X}_a &\mapsto \epsilon_a \mathcal{X}_a, \\
\mathcal{X}_b &\mapsto \epsilon_b \mathcal{X}_b, \\
\mathcal{X}_m &\mapsto \mathcal{X}_m,
\end{aligned} \tag{9.28}$$

for any choice of $\epsilon_a, \epsilon_b \in \{\pm 1\}$. Clearly this leaves the shear coordinates $\mathcal{Z}_E$ invariant (and hence leaves the $PSL(2)$-representation invariant), while changing the $SL(2)$-representation ρ.

9.3 Fenchel-Nielsen examples

Next we study the nonabelianization for Fenchel-Nielsen networks. We apply the construction to molecule I and II on the three-holed sphere, and also to Fenchel-Nielsen networks on the four-holed sphere and the genus two surface.

Let us note that, in principle, it would be enough to illustrate the procedure for three-holed spheres. We can obtain $\mathcal{W}$-pairs on any other surface by the gluing construction.

9.3.1 Pair of pants: molecule I

We start with the spectral network "molecule I" on the three-holed sphere. As always, we first specify the auxiliary data. Here we fix three basepoints for each double wall and a basis of simple paths $\wp_n$. Additionally, we fix a basepoint $z_{1,2,3}$ on each boundary component and assign a sheet ordering to each orientation of that boundary component. All choices are illustrated in Figure 34.

As before, we choose an $SL(2)$ matrix $\mathcal{D}_\wp$ for each simple path $\wp$. This matrix is diagonal if the path has an even number of intersections with branch cuts and strictly off-diagonal if this number is odd. In this example these matrices have 9 degrees of freedom

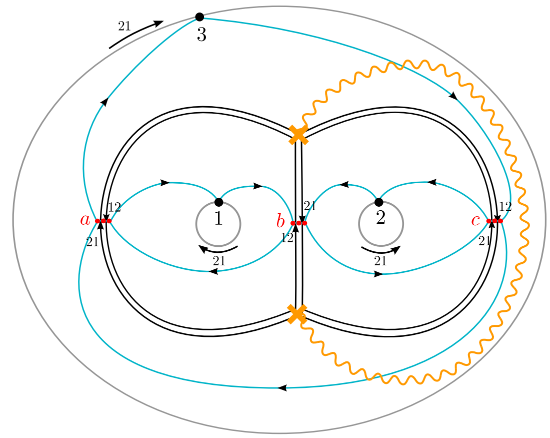

Figure 34: Molecule I with a marked point on each boundary (black dot), three basepoints for every double wall (red dots) and a collection of simple paths (blue lines). The boundary components are labeled as 1, 2 and 3 (in black) and the double walls as a, b and c (in red). The arrow on each boundary component indicates the sheet ordering in that orientation.

$d_\wp$. The collection of matrices $\mathcal{D}_\wp$ forms an equivariant $GL(1)$-representation ρ^{ab} iff the matrices obey the bulk constraints.

We choose a closed path $\gamma_{1,2,3}$ along each boundary component (in the same orientation as that of the boundary component), and enforce the $GL(1)$ holonomy along the lift $\gamma_{1,2,3}^{(ii)}$ to be equal to the ith diagonal entry of the matrix

$$M^{\mathrm{ab}}_{1,2,3} = \begin{pmatrix} \mathcal{X}_{1,2,3} & 0 \\ 0 & \mathcal{X}^{-1}_{1,2,3} \end{pmatrix}, \tag{9.29}$$

where $\mathcal{X}_{1,2,3} \neq 0, \pm 1$.[18] This gives three constraints on the nine unknowns $d_\wp$.

Abelian gauge transformations at the basepoints reduce the number of unknowns to three. The three remaining unknowns can be expressed in terms of parallel transport coefficients $\mathcal{X}_{12,23,31}$ along open paths that run from one boundary component to another. We can choose to additionally divide out by abelian gauge transformations at the marked points $z_{1,2,3}$, in which case the parallel transport coefficients drop out and the number of unknowns reduces to zero.

This gives a parametrization of all equivariant $GL(1)$-representations with boundary ρ_{ab} on the cover Σ. We now pick one and apply the non-abelianization construction.

We construct an $SL(2)$-representation from this $GL(1)$-representation by splicing in $\mathcal{S}$-matrices whenever the path $\wp$ crosses a wall. Requiring the resulting $SL(2)$-representation to be flat is equivalent to enforcing branch point constraints. There is one constraint for each branch point (see Figure 35). The $\mathcal{S}$-matrices are fully determined once we impose

[18] To restrict to irreducible representations we furthermore impose that $\mathcal{X}_1 \neq \mathcal{X}_2\mathcal{X}_3$, $\mathcal{X}_2 \neq \mathcal{X}_3\mathcal{X}_1$, $\mathcal{X}_3 \neq \mathcal{X}_1\mathcal{X}_2$ and $\mathcal{X}_1\mathcal{X}_2\mathcal{X}_3 \neq 1$. We find that these constraints translate to the constraints that we imposed when abelianizing Fenchel-Nielsen networks at the level of the image of the non-abelianization map (see for instance Proposition 3.2 in [25]).

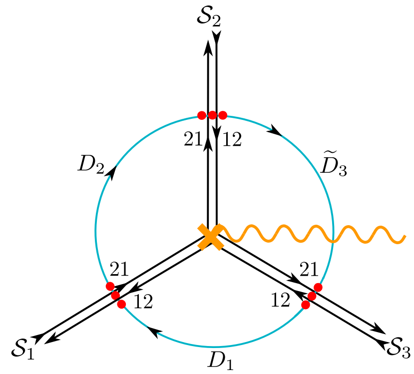

Figure 35: Local configuration around a branch point in a Fenchel-Nielsen network.

the branch point equations. For instance, consider the $\mathcal{S}$-matrix attached to the double wall (w_a^{21}, w_a^{12}) on the left in Figure 34. When crossing the double wall from the left to the right, this matrix can be written in the form

$$\mathcal{S}_a = \begin{pmatrix} 1 & 0 \\ S(w_a^{12}) & 1 \end{pmatrix} \begin{pmatrix} 1 & S(w_a^{21}) \\ 0 & 1 \end{pmatrix}, \tag{9.30}$$

with off-diagonal components

$$S(w_a^{12}) = \mathcal{X}(a_a^{12}) \left(\frac{1 + \mathcal{X}_b^2}{1 - \mathcal{X}_a^2 \mathcal{X}_b^2} \right) \tag{9.31}$$

$$S(w_a^{21}) = \mathcal{X}(a_a^{21}) \left(\frac{1 + \mathcal{X}_c^2}{1 - \mathcal{X}_a^2 \mathcal{X}_c^2} \right), \tag{9.32}$$

where we redefined $\mathcal{X}_1 = \mathcal{X}_a \mathcal{X}_b$, $\mathcal{X}_2 = \mathcal{X}_b \mathcal{X}_c$ and $\mathcal{X}_3 = \mathcal{X}_a \mathcal{X}_c$. The novel factor in these $\mathcal{S}$-matrices is an infinite sum of monomials in the coordinates $\mathcal{X}_{a,b,c}$.

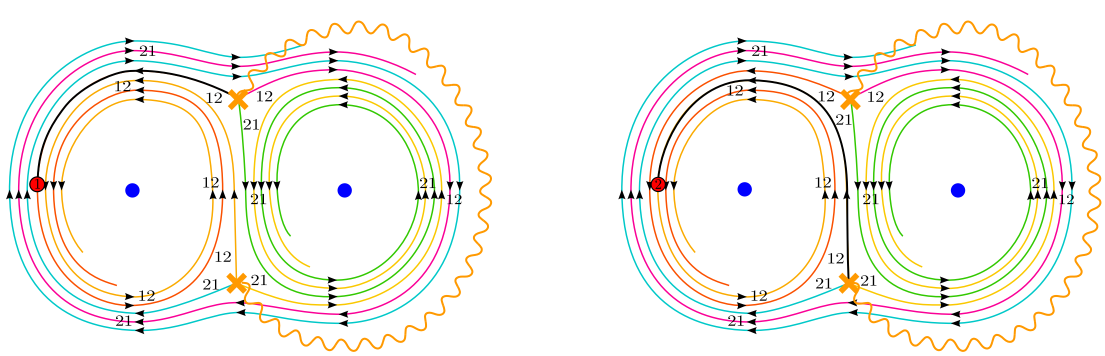

Figure 36: Left and right illustrate the interpretation of the terms $\mathcal{X}(a_a^{12})$ and $\mathcal{X}_b^2 \mathcal{X}(a_a^{12})$ in the $\mathcal{S}$-matrices, respectively, in the limiting spectral network to molecule II.

The interpretation for each monomial in the sum is best understood from the limiting spectral network illustrated in Figure 36. The term

$$\mathcal{X}(a_a^{12})$$

computes the abelian parallel transport along a path on Σ that starts at the red dot labeled by 1 (lifted to the second sheet of the cover), follows the (black part of the) orange wall to the upper branch point, circles around it, and runs back to the same red dot (lifted to the first sheet of the cover). The term

$$\mathcal{X}_b^2\, \mathcal{X}(a_a^{12})$$

computes the abelian parallel transport along a path that starts at the red dot labeled by 2 (lifted to the second sheet of the cover), follows the (black part of the) yellow wall all the way to the lower branch point, circles around it, and runs back to the same red dot (lifted to the first sheet of the cover). All other monomials in the $\mathcal{S}$-wall matrices can be explained similarly.

The $\mathcal{S}$-matrices attached to the two other double walls in the spectral network are obtained from $\mathcal{S}_a$ using the cyclic symmetry of the spectral network.

Length-twist coordinates

The resulting $SL(2)$-representation ρ has a diagonal monodromy matrix

$$\rho(\gamma_{1,2,3}) = \begin{pmatrix} \mathcal{X}_{1,2,3} & 0 \\ 0 & \mathcal{X}_{1,2,3}^{-1} \end{pmatrix} \tag{9.33}$$

along the closed paths $\gamma_{1,2,3}$. The $GL(1)$ holonomies $\mathcal{X}_{1,2,3}$ are each equal to a square-root of an exponentiated complex Fenchel-Nielsen length parameter. Thus we have found that these length parameters occur as an example of spectral parameters.

If we fix a trivialization of the equivariant $GL(1)$-representation at the marked points, the resulting $SL(2)$-representation ρ not only depends on the abelian holonomies $\mathcal{X}_{1,2,3}$, but also on the parallel transports $\mathcal{X}_{12,23,31}$ along open paths that begin and end on different boundary components. If we divide out by diagonal gauge transformations at the marked points the dependence on the parallel transport coefficients drops out.

We can furthermore reduce to $PSL(2)$-representations by considering transformations that map

$$(\mathcal{X}_1, \mathcal{X}_2, \mathcal{X}_3) \mapsto (\epsilon_1 \mathcal{X}_1, \epsilon_2 \mathcal{X}_2, \epsilon_3 \mathcal{X}_3), \tag{9.34}$$

for any choice of $(\epsilon_1, \epsilon_2, \epsilon_3) \in (\mathbb{Z}/2\mathbb{Z})^3$ satisfying $\epsilon_1\epsilon_2\epsilon_3 = 1$ (see also [25]). Let us call two equivariant $GL(1)$-representations $PSL(2)$-equivalent if they are related by such a transformation. Then we find a 1-1 correspondence between equivariant $GL(1)$-representations, up to $PSL(2)$ equivalence, and $PSL(2)$-representations.

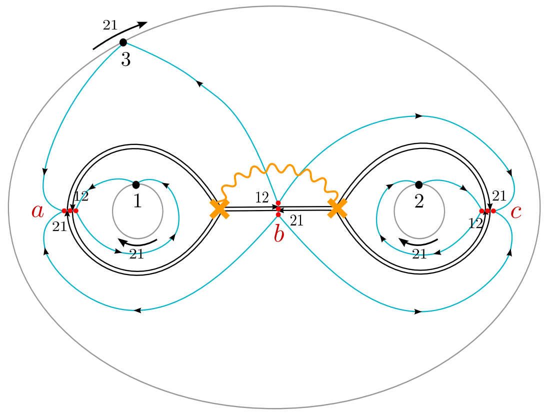

Figure 37: Molecule II with a marked point on each boundary (black dot), three basepoints for every double wall (red dots) and a collection of simple paths (blue lines). The boundary components are labeled as 1, 2 and 3 (in black) and the double walls as a, b and c (in red). The arrow on each boundary component indicates the sheet ordering in that orientation

9.3.2 Pair of pants: molecule II

The description of the nonabelianization map for molecule II is similar to that for molecule I. We can for instance determine it using the data in Figure 37. The off-diagonal components of the $\mathcal{S}$-matrices are functions of the $GL(1)$ holonomies $\mathcal{X}_{1,2,3}$ along closed paths $\gamma_{1,2,3}$ homotopic to the respective boundary components. If we redefine these parameters through the equations $\mathcal{X}_1 = \mathcal{X}_a$, $\mathcal{X}_2 = \mathcal{X}_c$ and $\mathcal{X}_3 = 1/(\mathcal{X}_a\mathcal{X}_b^2\mathcal{X}_c)$, the off-diagonal components are a series in the parameters $\mathcal{X}_{a,b,c}$. Crossing the 21-wall first and the 12-wall last, we have

$$\mathcal{S}_{a,b,c} = \begin{pmatrix} 1 & 0 \\ S(w^{12}_{a,b,c}) & 1 \end{pmatrix} \begin{pmatrix} 1 & S(w^{21}_{a,b,c}) \\ 0 & 1 \end{pmatrix}, \tag{9.35}$$

where

$$\begin{aligned} S(w_a^{12}) &= \mathcal{X}(a_a^{12})\frac{1}{(1-\mathcal{X}_a^2)} & S(w_a^{21}) &= \mathcal{X}(a_a^{21})\frac{(1+\mathcal{X}_b^2)(1+\mathcal{X}_c^2\mathcal{X}_b^2)}{1-\mathcal{X}_a^2\mathcal{X}_b^4\mathcal{X}_c^2} \\ S(w_b^{12}) &= \mathcal{X}(a_b^{12})\frac{1+\mathcal{X}_a^2(1+(1+\mathcal{X}_c^2)\mathcal{X}_b^2)}{1-\mathcal{X}_a^2\mathcal{X}_b^4\mathcal{X}_c^2} & S(w_b^{21}) &= \mathcal{X}(a_b^{21})\frac{1+\mathcal{X}_c^2(1+(1+\mathcal{X}_a^2)\mathcal{X}_b^2)}{1-\mathcal{X}_a^2\mathcal{X}_b^4\mathcal{X}_c^2} \\ S(w_c^{12}) &= \mathcal{X}(a_c^{12})\frac{1}{(1-\mathcal{X}_c^2)} & S(w_c^{21}) &= \mathcal{X}(a_c^{21})\frac{(1+\mathcal{X}_b^2)(1+\mathcal{X}_a^2\mathcal{X}_b^2)}{(1-\mathcal{X}_a^2\mathcal{X}_b^4\mathcal{X}_c^2)}. \end{aligned} \tag{9.36}$$

As the reader can verify, all monomials in the $\mathcal{S}$-matrices can be interpreted as abelian holonomies along auxiliary paths in the limiting network (which is illustrated in Figure 38).

9.3.3 Four-holed sphere

Given a pair of pants decomposition of the four-holed sphere, we can build a Fenchel-Nielsen type spectral network choosing either molecule I or II on each pair of pants. Let

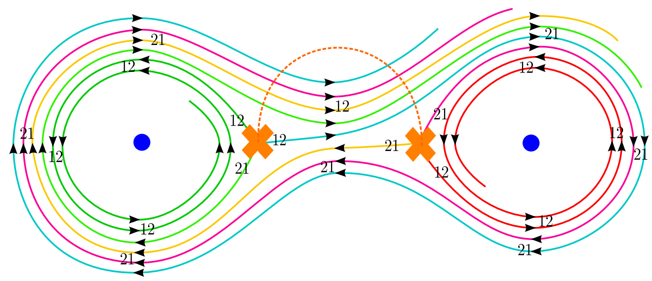

Figure 38: Limiting spectral network to molecule I.

us for instance determine the nonabelianization map for the spectral network illustrated in Figure 39, built by gluing two pairs of pants containing molecules of type II.

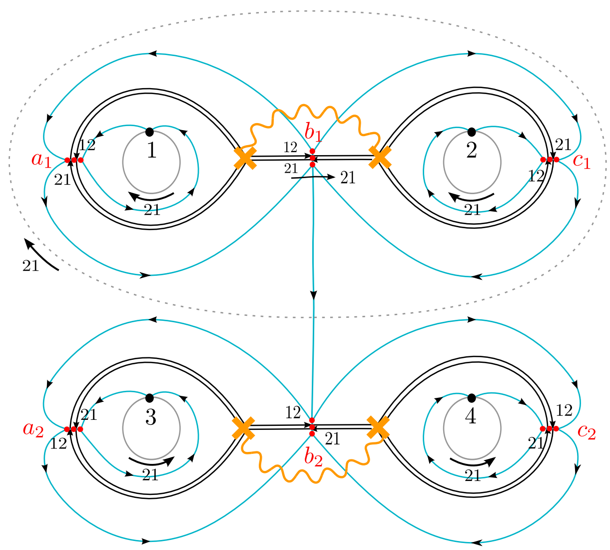

Figure 39: Fenchel-Nielsen spectral network on the four-holed sphere with a basepoint on each boundary (black dot), three basepoints for every double wall (red dots) and a collection of simple paths (blue lines). Additionally, an arrow denotes the sheet ordering in that direction on every boundary component and on the curve that defines the pants decomposition.

We fix basepoints and choose simple paths $\wp_{1\ldots 13}$ as illustrated in Figure 39. The matrices $\mathcal{D}_\wp$ thus contain 13 variables in total. The bulk constraints consist of boundary conditions at the boundaries and at infinity, and reduce the number of variables to 8. After fixing 6 abelian gauge degrees of freedom (one for each double wall), we are left with two gauge-invariant $GL(1)$ holonomies. Let us call these holonomies $\mathcal{X}_A$ and $\mathcal{X}_B$.

The cover Σ of the 4-holed sphere is an 8-holed torus. The $GL(1)$ holonomies $\mathcal{X}_{1,2,3,4}^{\pm 1}$ around the boundary components are part of the boundary conditions that we have just imposed. The coordinates $\mathcal{X}_A$ and $\mathcal{X}_B$ are abelian holonomies along a choice of 1-cycles A and B on the cover Σ that intersect each other once. To be explicit, let the 1-cycle A be a lift to sheet 1 of Σ of the 1-cycle α that defines the pants decomposition (see Figure 40).

We take B as the lift of a 1-cycle β in Figure 40, lifted and oriented in such a way that $A\#B = 1$.[19]

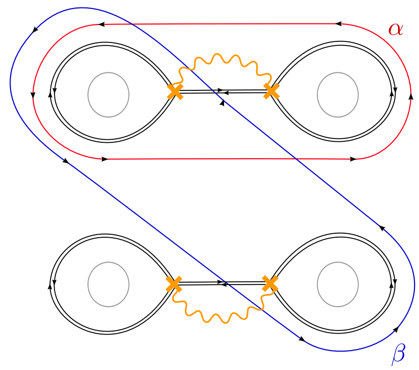

Figure 40: Choice of 1-cycles α and β on the four-holed sphere.

Having parametrized all equivariant $GL(1)$-representations on the cover Σ, we construct the corresponding nonabelian representations on the four-holed sphere by splicing in $\mathcal{S}$-matrices. These $\mathcal{S}$-matrices are completely determined by the non-abelian branch point equations. As can be expected from the gluing construction, we find that the $\mathcal{S}$-matrices are similar to those for the molecule II network on the three-holed sphere.

More precisely, the off-diagonal components of the $\mathcal{S}$-matrices for the top (bottom) molecule are equal to those in equation (9.36) after a change of variables

$$(\mathcal{X}_a, \mathcal{X}_b, \mathcal{X}_c) \mapsto (\mathcal{X}_{a_1}, \mathcal{X}_{b_1}, \mathcal{X}_{c_1})$$

(or $(\mathcal{X}_a, \mathcal{X}_b, \mathcal{X}_c) \mapsto (\mathcal{X}_{a_2}, \mathcal{X}_{b_2}, \mathcal{X}_{c_2})$), with $\mathcal{X}_1 = \mathcal{X}_{a_1}, \mathcal{X}_2 = \mathcal{X}_{c_1}, \mathcal{X}_3 = \mathcal{X}_{a_2}, \mathcal{X}_4 = \mathcal{X}_{c_2}$ and $\mathcal{X}_A = 1/(\mathcal{X}_{a_1}\mathcal{X}_{b_1}^2\mathcal{X}_{c_1}) = 1/(\mathcal{X}_{a_2}\mathcal{X}_{b_2}^2\mathcal{X}_{c_2})$.

Monodromy representations of the resulting $SL(2)$-representations can be expressed purely in terms of abelian data: the abelian holonomies $\mathcal{X}_{1,2,3,4}$ around the boundary components, the parallel transport coefficients along open paths that run from one boundary component to another and the abelian holonomies $\mathcal{X}_A$ and $\mathcal{X}_B$ around the 1-cycles A and B. If we divide out by diagonal gauge transformations at the marked points, the dependence on the parallel transport coefficients drops out.

Length-twist coordinates

The $SL(2)$ monodromy matrices around the loops α and $\mathcal{P}_{1,2,3,4}$ are all diagonal, of the form

$$\rho(\alpha, \mathcal{P}_{1,2,3,4}) = \begin{pmatrix} \mathcal{X}_{A,1,2,3,4} & 0 \\ 0 & \mathcal{X}_{A,1,2,3,4}^{-1} \end{pmatrix}. \tag{9.37}$$

The abelian holonomies $\mathcal{X}_{1,2,3,4,A}$ are equal to square-roots of the exponentiated, complexified Fenchel-Nielsen length parameters.

[19] We furthermore impose the constraints that $\mathcal{X}_{1,2,3,4,A} \neq 0, \pm 1$, and that when restricted to each pair of pants $\mathcal{X}_{i_1} \neq \mathcal{X}_{i_2}\mathcal{X}_{i_3}$, $\mathcal{X}_{i_2} \neq \mathcal{X}_{i_3}\mathcal{X}_{i_1}$, $\mathcal{X}_{i_3} \neq \mathcal{X}_{i_1}\mathcal{X}_{i_2}$ and $\mathcal{X}_{i_1}\mathcal{X}_{i_2}\mathcal{X}_{i_3} \neq 1$. These constraint are equivalent to the constraints that we imposed when abelianizing with Fenchel-Nielsen networks [25].

In particular, we have found that the spectral coordinate $\mathcal{X}_A$ is the square-root of the exponentiated, complexified Fenchel-Nielsen length coordinate. Much less trivial from this construction is that the spectral coordinate $\mathcal{X}_B$ is the exponential of a complexified Fenchel-Nielsen twist parameter.

We verify this claim by comparing the traces of the monodromy matrices for ρ with a complex version of Okai's formula, which computes these traces in terms of the Fenchel-Nielsen twist parameter [26]. (We also found it helpful to look at Kabaya's analysis in [25], in which a set of matrix generators of $SL(2)$ flat connections is systemetically found in terms of a complexified version of the Fenchel-Nielsen coordinates and compared to Okai's formula for Fuchsian representations.) Let us consider the monodromy matrix M_β along the loop β, illustrated in Figure 40.

On the one hand, Okai's formula computes the trace of this monodromy as

$$\mathrm{Tr}\, M_\beta = \sqrt{c}\left(\frac{t}{\mathcal{X}_A} + \frac{\mathcal{X}_A}{t}\right) + d, \tag{9.38}$$

in terms of the Fenchel-Nielsen twist parameter t. The coefficients c and d are given by

$$\begin{aligned} c &= \frac{1}{(\mathcal{X}_A - \mathcal{X}_A^{-1})^4}\left(\mathcal{Z}_A^2 + \mathcal{Z}_1^2 + \mathcal{Z}_2^2 - \mathcal{Z}_A\mathcal{Z}_1\mathcal{Z}_2 - 4\right)\left(\mathcal{Z}_A^2 + \mathcal{Z}_3^2 + \mathcal{Z}_4^2 - \mathcal{Z}_A\mathcal{Z}_3\mathcal{Z}_4 - 4\right) \\ d &= \frac{1}{(\mathcal{X}_A - \mathcal{X}_A^{-1})^2}\left(\mathcal{Z}_A(\mathcal{Z}_2\mathcal{Z}_4 + \mathcal{Z}_1\mathcal{Z}_3) - 2(\mathcal{Z}_1\mathcal{Z}_4 + \mathcal{Z}_2\mathcal{Z}_3)\right), \end{aligned}$$

and $\mathcal{Z}_A = \mathcal{X}_A + \mathcal{X}_A^{-1}$ and $\mathcal{Z}_p = \mathcal{X}_p + \mathcal{X}_p^{-1}$.

On the other hand, the trace of the monodromy matrix M_β of the $SL(2)$-representation ρ is given by

$$\mathrm{Tr}\, M_\beta = -\left(\mathcal{X}_B + \frac{c}{\mathcal{X}_B}\right) + d. \tag{9.39}$$

Comparing the two formulas we conclude that

$$t = -\left(\frac{\mathcal{X}_A}{\sqrt{c}}\right)\mathcal{X}_B. \tag{9.40}$$

In other words, the spectral coordinate $\mathcal{X}_B$ is the exponential of a complexified version of a Fenchel-Nielsen twist coordinate.

Even though the precise form of the multiplicative factor depends on characteristics of the chosen Fenchel-Nielsen network, we find that the spectral coordinate $\mathcal{X}_B$ is always proportional to the Fenchel-Nielsen parameter t.

Of course, in this comparison we have to be careful to match the $SL(2)$ monodromies around the same 1-cycle β. If we compute the $SL(2)$ monodromy along any other choice of 1-cycle β' that intersects the 1-cycle α once, equation (9.39) holds in a modified form

$$\mathrm{Tr}\, M_{\beta'} = -\left(\mathcal{X}_{B'} + \frac{c'}{\mathcal{X}_{B'}}\right) + d', \tag{9.41}$$

where B' is a lift of β' to the covering (following the same rules as before). For any such choice we find that the abelian holonomy $\mathcal{X}_{B'}$ is a twist coordinate (by comparing to formulae in [26, 25]).

We can further reduce to $PSL(2)$-representations by dividing out the transformations

$$(\mathcal{X}_1, \mathcal{X}_2, \mathcal{X}_a, \mathcal{X}_4, \mathcal{X}_5) \mapsto (\epsilon_1 \mathcal{X}_1, \epsilon_2 \mathcal{X}_2, \epsilon_a \mathcal{X}_a, \epsilon_4 \mathcal{X}_4, \epsilon_5 \mathcal{X}_5), \tag{9.42}$$

where $\epsilon_I = \pm 1$ with the constraints that $\epsilon_1 \epsilon_2 \epsilon_a = 1$ as well as $\epsilon_a \epsilon_4 \epsilon_5 = 1$ [25].[20]

9.3.4 Genus 2 surface

Finally we consider the case of a genus 2 surface. We choose the Fenchel-Nielsen network and the auxiliary data as shown in Figure 41. Our goal is to check directly that the 6 Fenchel-Nielsen length and twist coordinates occur as spectral coordinates.

Let us first verify that there is indeed a 6-parameter family of equivariant $GL(1)$-representations ρ^{ab}. There are 15 simple paths $\wp$ and 3 nontrivial flatness conditions. Furthermore, there are 6 gauge redundancies (one for each double wall). This leaves us with 6 gauge-invariant abelian holonomies. These can be associated to holonomies along six 1-cycles $A_{1,2,3}$ and $B_{1,2,3}$ on the cover Σ of the genus two surface, with $A_i \# B_j = \delta_{ij}$.[21] To be explicit, these 1-cycles are lifts of 1-cycles $\alpha_{1,2,3}$ and $\beta_{1,2,3}$ on the genus two surface, which we choose in a way analogous to what we did in the four-holed sphere example. That is, we identify each tube in the pants decomposition of the genus 2 surface with the internal tube of a four-holed sphere, and then choose the 1-cycles α_k and β_k for this tube as shown in Figure 40.

As in previous examples, we can solve for the $\mathcal{S}$-matrices uniquely (by imposing the branch point equations as well fixing the eigenvalues of the non-abelian monodromies around the tubes), and, as can be expected from the gluing construction, we find that they are of the form (9.35). It is immediate that the complexified Fenchel-Nielsen length coordinates match the spectral coordinates $\mathcal{X}_{A_{1,2,3}}$. To find the Fenchel-Nielsen twist coordinates we compute the $SL(2)$ monodromies around the cycles $\beta_{1,2,3}$. We have carried out this computation, and find that the spectral coordinates $\mathcal{X}_{B_{1,2,3}}$ are indeed complexified Fenchel-Nielsen twist coordinates. (Similar to formula (9.40) they agree with the Fenchel-Nielsen twist parameter in section 12.4 of [25] up to a multiplicative term).

9.4 Mixed networks

Just as for Fenchel-Nielsen and Fock-Goncharov type networks, we can apply the nonabelianization map to any mixed type spectral network. In particular, for the examples discussed in §2, we find unique solutions for the $\mathcal{S}$-matrices. The off-diagonal elements in these solutions have a similar interpretation in the limiting network as abelian holonomies along auxiliary paths on Σ.

[20] Here one has to be careful that the action of the group $(\mathbb{Z}/2\mathbb{Z})^3$ on $\mathcal{X}_B$ is not trivial (since B is not an even cycle). Instead $\mathcal{X}_B$ transforms in the same way as the factor d. The action of $(\mathbb{Z}/2\mathbb{Z})^3$ *is* trivial on the twist parameter $\tilde{t} = \sqrt{\frac{(\mathcal{X}_a\mathcal{X}_1 - \mathcal{X}_2)(1-\mathcal{X}_1\mathcal{X}_2\mathcal{X}_a)(\mathcal{X}_a\mathcal{X}_5-\mathcal{X}_4)(1-\mathcal{X}_a\mathcal{X}_4\mathcal{X}_5)}{(\mathcal{X}_a\mathcal{X}_2-\mathcal{X}_1)(\mathcal{X}_1\mathcal{X}_2-\mathcal{X}_a)(\mathcal{X}_a\mathcal{X}_4-\mathcal{X}_5)(\mathcal{X}_4\mathcal{X}_5-\mathcal{X}_a)}}\, t$.

[21] There are ten 1-cycles on the genus 5 cover, but the holonomies of an equivariant $GL(1)$-connection around these 1-cycles are not all independent: $\mathcal{X}(\sigma^*\gamma) = \mathcal{X}(\gamma)^{-1}$.

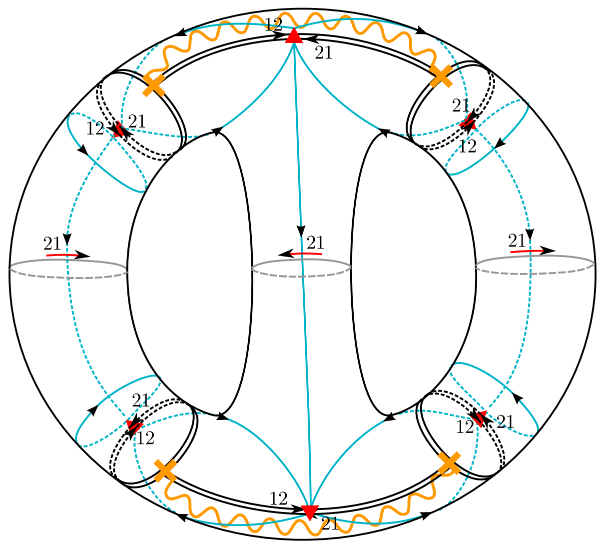

Figure 41: Example of a Fenchel-Nielsen network on the genus two surface, together with a choice of auxiliary data: branch-cut (orange wigly lines), basepoints (red triangles), short paths (light blue lines) and a sheet ordering for every orientation of the pants curves.

Using this explicit form of the $\mathcal{S}$-matrices, we obtain $SL(2)$-representations in terms of purely abelian data. We can compute a monodromy representation in terms of the spectral coordinates, and compare to known coordinate systems. We have done this, and found that not all spectral coordinates for mixed spectral networks can be expressed as Fenchel-Nielsen or Fock-Goncharov coordinates. We leave the further exploration of these coordinates for future work.

10 Some consequences

10.1 Asymptotics

One of the most interesting properties of the spectral coordinates [1] is that they have simple asymptotics when evaluated along certain natural one-parameter families of $SL(2)$-connections. This asymptotic property was described in [3] in the case of Fock-Goncharov spectral networks. One consequence of the constructions described in this paper is that a similar asymptotic property should hold for Fenchel-Nielsen coordinates. In this section we briefly describe that story.

We will consider one-parameter families of flat $SL(2)$-connections, $\{\nabla(\zeta)\}_{\zeta\in\mathbb{C}^\times}$. We will not consider arbitrary families, but rather only the ones which come from solutions of Hitchin equations. These equations concern a tuple (E, D, φ) where E is a Hermitian rank 2 bundle over C, D a (generally non-flat) unitary connection in E, and φ a section of $\Omega^{1,0}(\mathrm{End}\, E)$. The equations are:

$$F_D + [\varphi, \varphi^\dagger] = 0, \tag{10.1}$$

$$\bar{\partial}_D \varphi = 0. \tag{10.2}$$

The moduli of solutions of these equations was studied in [27], and in [28] this analysis was extended to the case where D and φ are allowed to have first-order poles. This is the case relevant for us.

Given a solution of Hitchin's equations, the corresponding family of flat (non-unitary) connections is

$$\nabla(\zeta) = \zeta^{-1}\varphi + D + \zeta\varphi^{\dagger}. \tag{10.3}$$

Indeed Hitchin's equations say precisely that the connection $\nabla(\zeta)$ is flat for every $\zeta \in \mathbb{C}^{\times}$.

Now we ask: how does $\nabla(\zeta)$ behave asymptotically as $\zeta \to 0$? The answer to this question is somewhat intricate; in particular, it turns out to depend on precisely how ζ approaches 0. One can get simpler answers if one restricts ζ to lie in a half-plane, say the open half-plane $\mathcal{H}_\vartheta$ centered on the ray $e^{\mathrm{i}\vartheta}\mathbb{R}_+$, and if one chooses the correct coordinate system on the moduli of flat connections. Namely, given the Higgs field φ, we consider the quadratic differential

$$\varphi_2 = \mathrm{Tr}(e^{-2\mathrm{i}\vartheta}\varphi^2). \tag{10.4}$$

Because φ has only first-order poles, φ_2 has at most second-order poles. Moreover, if φ is chosen generically, then φ_2 has only simple zeroes; we assume that from now on. As described in §3, the quadratic differential φ_2 corresponds to a particular spectral curve $\Sigma \subset T^*C$ and spectral network $\mathcal{W}(\varphi_2)$. This spectral network induces spectral coordinate functions $\mathcal{X}_\gamma$. The $\zeta \to 0$ asymptotics of the spectral coordinates of the family $\nabla(\zeta)$ were studied in [3, 1], where it was argued that they are controlled by the periods of the spectral curve:

$$\mathcal{X}_\gamma(\nabla(\zeta)) \sim c_\gamma \exp\left(\zeta^{-1}\oint_\gamma \lambda\right) \tag{10.5}$$

where c_γ is ζ-independent, and λ denotes the tautological (Liouville) 1-form on T^*C.

In particular, suppose φ is a generic Higgs field, so that φ_2 is a generic quadratic differential. In this case the spectral network $\mathcal{W}(\varphi_2)$ is a Fock-Goncharov network, and the corresponding coordinates are Fock-Goncharov coordinates. Thus (10.5) tells us the asymptotic behavior of the Fock-Goncharov coordinates of the connections $\nabla(\zeta)$. These asymptotics were derived using the WKB method in [3], and a more general method of obtaining them was described in [1].

On the other hand, suppose that φ is a special Higgs field, such that φ_2 is a Strebel differential. In this case $\mathcal{W}(\varphi_2)$ is a Fenchel-Nielsen network, and (10.5) tells us the asymptotic behavior of the Fenchel-Nielsen coordinates of $\nabla(\zeta)$. (More precisely, the spectral coordinates associated to $\mathcal{W}(\varphi_2)$ depend on whether we take the British or American resolution; the asymptotics (10.5) in the open half-plane $\mathcal{H}_\vartheta$ apply to either. We believe that for the British resolution the asymptotics extend also to one of the rays on the *boundary* of the half-plane, and for the American resolution they extend to the other boundary. It would be useful to verify this by direct application of the WKB method.)

Remember that the periods $\oint_\gamma \lambda$ are real-valued when φ_2 is a Strebel differential and γ is the lift to Σ of a pants curve on C. The Fenchel-Nielsen length coordinates thus behave asymptotically as the exponentials of a set of real period integrals. This makes precise the identification between Coulomb parameters and length coordinates that follows from the AGT correspondence.

10.2 Line defects

A second interesting consequence of our discussion concerns the physics of line defects.

Recall from [29, 30] that, in the theory $S[A_1, C]$ associated to a punctured Riemann surface C, there is a class of supersymmetric line defects $L(\wp, \zeta)$ labeled by closed loops $\wp$ on C and phases $\zeta \in \mathbb{C}^\times$.

According to [30], the spectrum of framed BPS states attached to $L(\wp, \zeta)$ can be read off from the abelianization map, as follows. Let M denote the holonomy of an $SL(2)$-connection around $\wp$. Given any spectral network $\mathcal{W}$, the $\mathcal{W}$-abelianization map expresses $\operatorname{Tr} M$ as a sum of $GL(1)$ holonomies

$$\operatorname{Tr} M = \sum_\gamma \overline{\underline{\Omega}}(\wp, \gamma, \mathcal{W}) \mathcal{X}_\gamma, \tag{10.6}$$

where the coefficients $\overline{\underline{\Omega}}(\wp, \gamma, \mathcal{W}) \in \mathbb{Z}$. If $\mathcal{W}$ is the WKB spectral network corresponding to a quadratic differential φ_2/ζ^2, then these coefficients have a physical interpretation: $\overline{\underline{\Omega}}(\wp, \gamma, \mathcal{W})$ counts the framed BPS states of charge γ attached to the line defect $L(\wp, \zeta)$, at the point of the Coulomb branch determined by φ_2.

If φ_2 is generic, and $\wp$ is not a cycle contractible to a puncture, this always leads to at least three framed BPS states. However, if $\mathcal{W}$ happens to be a Fenchel-Nielsen network, or more generally a mixed network whose complement contains at least one annulus A, then we may take $\wp$ to be a path going around A. In this case, $\mathcal{W}$-abelianization for $\wp$ is very simple: $\wp$ crosses no walls at all, so

$$\operatorname{Tr} M = \mathcal{X}_\gamma + \mathcal{X}_{-\gamma} \tag{10.7}$$

where γ and $-\gamma$ are the two lifts of $\wp$ to the double cover Σ. Thus, in this situation the supersymmetric line defect $L(\gamma, \zeta)$ supports just two framed BPS states, carrying charges γ, $-\gamma$.

Physically we would interpret this in the following way. Let us choose a particular way of looking at the theory $S[A_1, C]$, in which this theory is obtained by gauging a particular $SU(2)$ symmetry in another theory $S[A_1, C']$, with C' obtained from C by cutting along the annulus A. From this point of view, the line defect $L(\wp, \zeta)$ is a Wilson line for the new $SU(2)$ gauge symmetry, in the fundamental representation. Naive classical reasoning would suggest that in the IR this defect should support two framed BPS states, corresponding to the decomposition of the fundamental representation into two weight spaces under $U(1) \subset SU(2)$. At generic (φ_2, ζ) this classical reasoning is not exactly correct: we do get these two states but we get additional states as well. What we have found here is that, if (φ_2, ζ) are chosen specially, the classical picture is precisely correct. (See also some related discussion in [31]).

It would be very interesting to have a direct physical understanding of *why* this simplification occurs.

References

[1] D. Gaiotto, G. W. Moore, and A. Neitzke, "Spectral networks," *Annales Henri Poincare* **14** (2013) 1643–1731, 1204.4824.

[2] D. Gaiotto, "N=2 dualities," *JHEP* **08** (2012) 034, 0904.2715.

[3] D. Gaiotto, G. W. Moore, and A. Neitzke, "Wall-crossing, Hitchin Systems, and the WKB Approximation," 0907.3987.

[4] D. Gaiotto, G. W. Moore, and A. Neitzke, "Spectral Networks and Snakes," *Annales Henri Poincare* **15** (2014) 61–141, 1209.0866.

[5] D. Galakhov, P. Longhi, T. Mainiero, G. W. Moore, and A. Neitzke, "Wild Wall Crossing and BPS Giants," *JHEP* **11** (2013) 046, 1305.5454.

[6] K. Hori, C. Y. Park, and Y. Tachikawa, "2d SCFTs from M2-branes," *JHEP* **11** (2013) 147, 1309.3036.

[7] K. Maruyoshi, C. Y. Park, and W. Yan, "BPS spectrum of Argyres-Douglas theory via spectral network," 1309.3050.

[8] T. Aoki, T. Kawai, S. Sasaki, A. Shudo, and Y. Takei, "Virtual turning points and bifurcation of Stokes curves for higher order ordinary differential equations," *J. Phys. A* **38** (2005), no. 15, 3317–3336, math-ph/0409005.

[9] V. Fock and A. Goncharov, "Moduli spaces of local systems and higher Teichmüller theory," *Publ. Math. Inst. Hautes Études Sci.* (2006), no. 103, 1–211, math/0311149.

[10] W. Fenchel and J. Nielsen, "Discontinuous groups of isometries in the hyperbolic plane," *de Gruyter Studies in Mathematics* **29** (2003).

[11] S. Wolpert, "The length spectra as moduli for compact Riemann surfaces," *Annals of Maths* **109** (1979) 323–351.

[12] S. Wolpert, "The Fenchel-Nielsen deformation," *Annals of Maths* **115** (1982) 501–528.

[13] C. Kourouniotis, "Complex length coordinates for quasi–Fuchsian groups," *Mathematika* **41** (1994) 173–188.

[14] S. P. Tan, "Complex Fenchel–Nielsen coordinates for quasi-Fuchsian structures," *Internat. J. Math.* **5** (1994) 239–251.

[15] N. Nekrasov, A. Rosly, and S. Shatashvili, "Darboux coordinates, Yang-Yang functional, and gauge theory," *Nucl. Phys. Proc. Suppl.* **216** (2011) 69–93, 1103.3919.

[16] E. Witten, "Solutions of four-dimensional field theories via M-theory," *Nucl. Phys.* **B500** (1997) 3–42, hep-th/9703166.

[17] L. F. Alday, D. Gaiotto, and Y. Tachikawa, "Liouville Correlation Functions from Four-dimensional Gauge Theories," *Lett. Math. Phys.* **91** (2010) 167–197, 0906.3219.

[18] J. Teschner, "Quantization of the Hitchin moduli spaces, Liouville theory, and the geometric Langlands correspondence I," *Adv.Theor.Math.Phys.* **15** (2011) 471–564, 1005.2846.

[19] V. Pestun, "Localization of gauge theory on a four-sphere and supersymmetric Wilson loops," *Commun.Math.Phys.* **313** (2012) 71–129, 0712.2824.

[20] J. Liu, “JenkinsStrebel differentials with poles,” *Comment. Math. Helv.* **83** (2008) 211–240.

[21] J. Hubbard and H. Masur, “Quadratic differentials and foliations,” *Acta Mathematica* **142** (1979) 221–274.

[22] V. V. Fock and A. A. Rosly, “Poisson structure on moduli of flat connections on Riemann surfaces and r-matrix,” math.QA/9802054.

[23] M. F. Atiyah and R. Bott, “The Yang-Mills equations over Riemann surfaces,” *Philos. Trans. Roy. Soc. London Ser. A* **308** (1983), no. 1505, 523–615.

[24] V. Fock, “Dual Teichmüller spaces,” *Am. Math. Soc. Transl.* **191** (1999) 67–86, dg-ga/9702018.

[25] Y. Kabaya, “Parametrization of PSL(2,C)–representations of surface groups,” *Geometriae Dedicata* **170, Issue 1** (2011) 9–62, 1110.6674.

[26] T. Okai, “Effects of a change of pants decompositions on their Fenchel–Nielsen coordinates,” *Kobe J. Maths.* **10** (1993) 215–223.

[27] N. J. Hitchin, “The self-duality equations on a Riemann surface,” *Proc. London Math. Soc. (3)* **55** (1987), no. 1, 59–126.

[28] C. Simpson, “Harmonic bundles on noncompact curves,” *J. Amer. Math. Soc.* **3** (1990) 713–770.

[29] N. Drukker, D. R. Morrison, and T. Okuda, “Loop operators and S-duality from curves on Riemann surfaces,” *JHEP* **09** (2009) 031, 0907.2593.

[30] D. Gaiotto, G. W. Moore, and A. Neitzke, “Framed BPS States,” *Adv. Theor. Math. Phys.* **17** (2013), no. 2, 241–397, 1006.0146.

[31] C. Cordova and A. Neitzke, “Line Defects, Tropicalization, and Multi-Centered Quiver Quantum Mechanics,” *JHEP* **09** (2014) 099, 1308.6829.